AFFDL-TR-69-36

C-1

CALIBRATION OF THE AFFDL 50 MEGAWATT ARC HEATED HYPERSONIC WIND TUNNEL WITH A TWO-FOOT NOZZLE

JAMES L. FOLCK
RICHARD T. SMITH

TECHNICAL REPORT AFFDL-TR-69-36

AUGUST 1969

AIR FORCE FLIGHT DYNAMICS LABORATORY
AIR FORCE SYSTEMS COMMAND
WRIGHT-PATTERSON AIR FORCE BASE, OHIO

NOTICE

When Government drawings, specifications, or other data are used for any purpose other than in connection with a definitely related Government procurement operation, the United States Government thereby incurs no responsibility nor any obligation whatsoever; and the fact that the government may have formulated, furnished, or in any way supplied the said drawings, specifications, or other data, is not to be regarded by implication or otherwise as in any manner licensing the holder or any other person or corporation, or conveying any rights or permission to manufacture, use, or sell any patented invention that may in any way be related thereto.

Copies of this report should not be returned unless return is required by security considerations, contractual obligations, or notice on a specific document.

500 - September 1969 - CO455 - 91-1999

AFFDL-TR-69-36

CALIBRATION OF THE AFFDL 50 MEGAWATT ARC HEATED HYPERSONIC WIND TUNNEL WITH A TWO-FOOT NOZZLE

JAMES L. FOLCK

RICHARD T. SMITH

FOREWORD

This report was prepared by Richard T. Smith and James L. Folck of the Electrogasdynamics Branch (FDME), Flight Mechanics Division, Air Force Flight Dynamics Laboratory, Wright-Patterson Air Force Base, Ohio. The work was conducted under Project No. 1426, "Experimental Simulation for Flight Mechanics," Task No. 142612, "50 Megawatt Electrogasdynamics Facility."

The work was accomplished during the period September 1967 to December 1968. The report was submitted by the authors in March 1969.

This technical report has been reviewed and is approved.

Philip P. Antonatos

PHILIP P. ANTONATOS
Chief, Flight Mechanics Division
Air Force Flight Dynamics Laboratory

ABSTRACT

This study consisted of the experimental investigation of test flow in an arc heated hypersonic wind tunnel. These tests utilized a high voltage DC arc heater which operated at input powers in excess of 50 megawatts and provided reservoir pressures ranging from 100 to 1500 psi and bulk enthalpies from 1500 to 4000 BTU/lb. Local free stream measurements of pitot pressure, mass flux, stagnation point heat transfer rate and wall static pressures were obtained at the exit of a nominal two-foot diameter conical nozzle. Stagnation enthalpy profiles at the nozzle exit became peaked at high stagnation pressures. From these data, center line enthalpies as high as 6500 BTU/lb were indicated in the flow. Selective comparisons between one-dimensional expansion theory and experiment are presented. At a reservoir enthalpy of approximately 2500 BTU/lb and for stagnation pressures in excess of 500 psi the expanded flow data were in good agreement with equilibrium expansion theory. However, below 500 psi the data compared more closely with nonequilibrium theory with the flow frozen downstream of the nozzle throat.

TABLE OF CONTENTS

ILLUSTRATIONS

ILLUSTRATIONS (CONTD)

SYMBOLS

A	area, ft^2
A^*	throat area, ft^2
C_p	specific heat at constant pressure
d	geometric diameter
E	voltage
H, h	enthalpy, BTU/lb
I	current, amperes
Le	Lewis number
$\dot{m}$	water flow rate, lb/sec
P	pressure, psia
Pr	Prandtl number
P_v^b	vacuum pump inlet pressure when P_∞ is 50% larger than its value at fully expanded nozzle flow, i.e., flow collapsed
P_{T_2}	pitot pressure, mm Hg
$\dot{q}$	heat transfer rate, BTU/ft^2-sec
$\dot{Q}$	gas stream energy, BTU/sec
R, r	radius, Reynolds number, gas constant
S	entropy
T	temperature
ΔT	temperature change
u	velocity, ft/sec
X, L	characteristic length
α	degree of dissociation
γ	ratio of specific heats
δ^*	boundary layer displacement thickness

SYMBOLS (CONTD)

η	efficiency, %
μ	viscosity
ρ	density, lb/ft^3
$\dot{\omega}$	air mass flow rate, lb/sec

Subscripts

d	dissociation, diffuser
esf	equilibrium sonic flow
f	freezing conditions
F & R	Fay and Riddell theory
HB	heat balance
H_2O	water property
M	model
o	stagnation conditions
r	reference conditions
s	local stagnation conditions
w	conditions at wall
∞	free stream conditions

SECTION I

INTRODUCTION

Arc heated hypersonic wind tunnels play an important role in today's aerospace technology. These facilities are required to study aerodynamic heating and ablation characteristics associated with hypersonic cruise and reentry vehicles. This type of an investigation requires an extreme hyperthermal environmental facility capable of operating on a continuous basis. The arc heater is one of the best available means of establishing these reservoir conditions.

Because of high stagnation temperatures produced in the arc chamber, the vibrational energy modes of the gas molecules become excited and an appreciable amount of dissociation occurs. As the gas is expanded through a nozzle the changes in temperature and density are sufficiently rapid that the recombination and vibration de-excitation reaction processes cannot equilibrate. The resultant thermal and chemical nonequilibrium gas state is characterized by a reduction in the velocity, static pressure, and temperature as compared to an equilibrium expansion. Studies (References 1 through 4) of a nonequilibrium expansion process have been made using an inviscid, one-dimensional, chemically reacting gas model. To date, however, no successful attempt has been made in coupling the nonequilibrium expansion with a realistic boundary layer calculation. Therefore, until this is accomplished, these programs cannot be used to predict arc heater-nozzle performance. Thus before meaningful aerodynamic and thermodynamic testing can be accomplished in an arc-heated facility, the important test section flow parameters must be experimentally determined. Several plasma diagnostic studies have been reported (References 5 through 8) yet the study presented here is the most complete calibration of an arc heated hypersonic wind tunnel which has been accomplished to date. Local free stream measurements of pitot pressure, mass flux, stagnation point heat transfer rate, and wall static pressure have been made and selective comparisons between theory and experiment are presented.

SECTION II

DESCRIPTION OF EQUIPMENT AND INSTRUMENTATION

1. GENERAL FACILITY DESCRIPTION

These tests were conducted in the Air Force Flight Dynamics Laboratory 50 Megawatt Electrogasdynamics Facility which is a continuous flow, electric arc-heated hypersonic wind tunnel. A sketch of the overall facility complex is shown in Figure 1. A schematic of an arc heated wind tunnel, shown in Figure 2, better describes the functional relation of the primary components. High pressure air is injected into the arc heater where the air is heated to very high stagnation temperatures. The air is then expanded in the nozzle to hypersonic conditions at the test section. The flow then passes through the diffuser, several banks of heat exchangers, and is recompressed to ambient pressure through several stages of vacuum pumps and exhausted to the atmosphere. The test cabin of the facility is equipped with a probe strut which can be traversed longitudinally and radially across the nozzle exit. A complete description of this facility including estimated performance characteristics is given in Reference 9.

2. ARC HEATER AND NOZZLE

The arc heater is a high pressure, high voltage design which was developed by the Air Force Flight Dynamics Laboratory and described in detail in References 10 and 11. The arc heater consists of two coaxial tubular electrodes attached to a centrally located air injection chamber shown in Figure 3. Air, metered through a calibrated ASME orifice, is injected tangentially into the heater which induces a vortex flow to stabilize the arc and rotate the arc attachment points. The front electrode terminates at the nozzle throat. Pressure taps located in the rear of the heater and in the swirl chamber are used to measure the arc heater pressure. These tests were conducted using a 16-degree included angle conical nozzle with one- and two-inch diameter interchangeable throats and a 25.2-inch exit diameter. The nozzle is instrumented with wall static pressure taps at several locations near the exit.

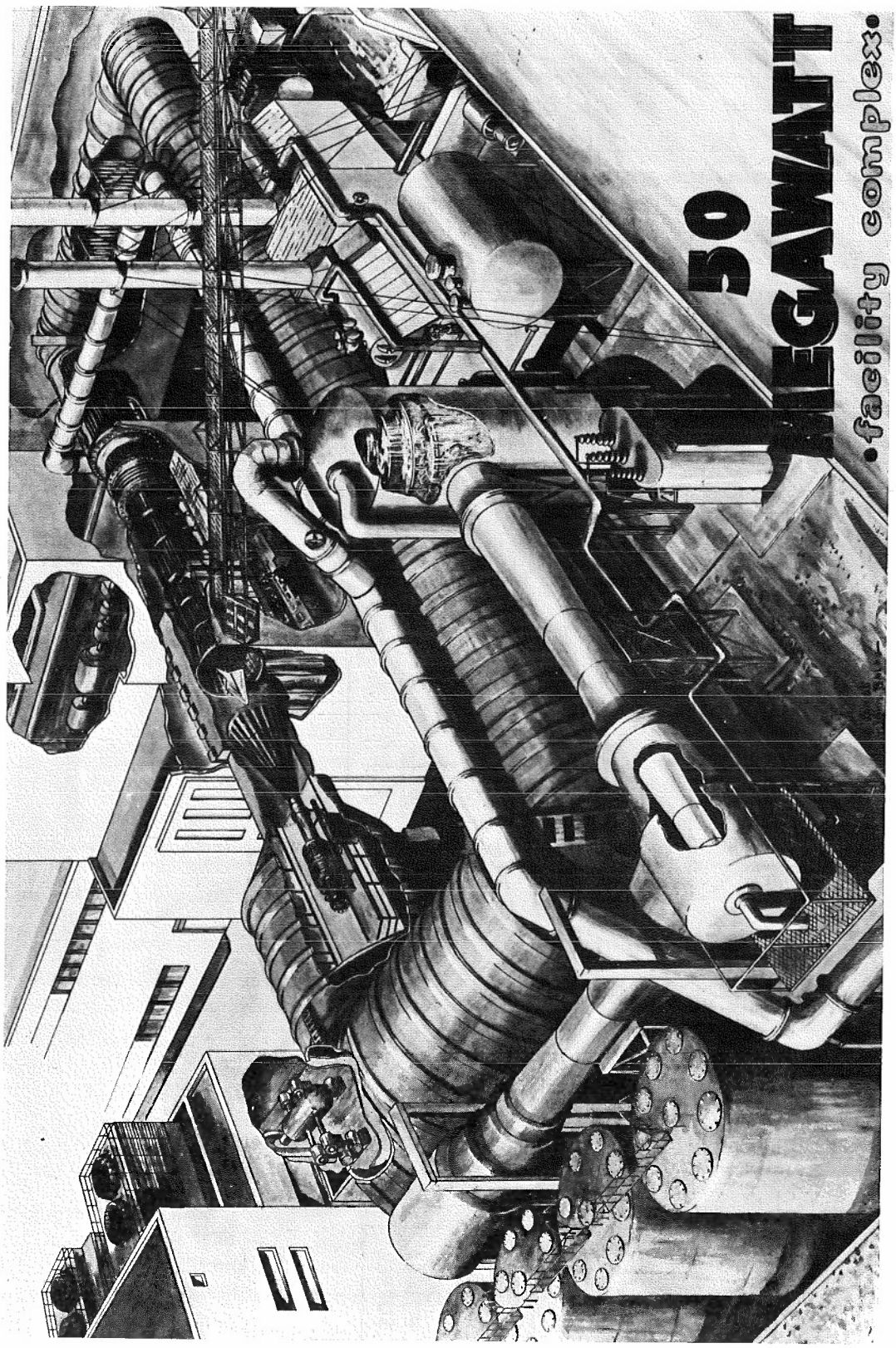

Figure 1. 50 Megawatt Facility Complex

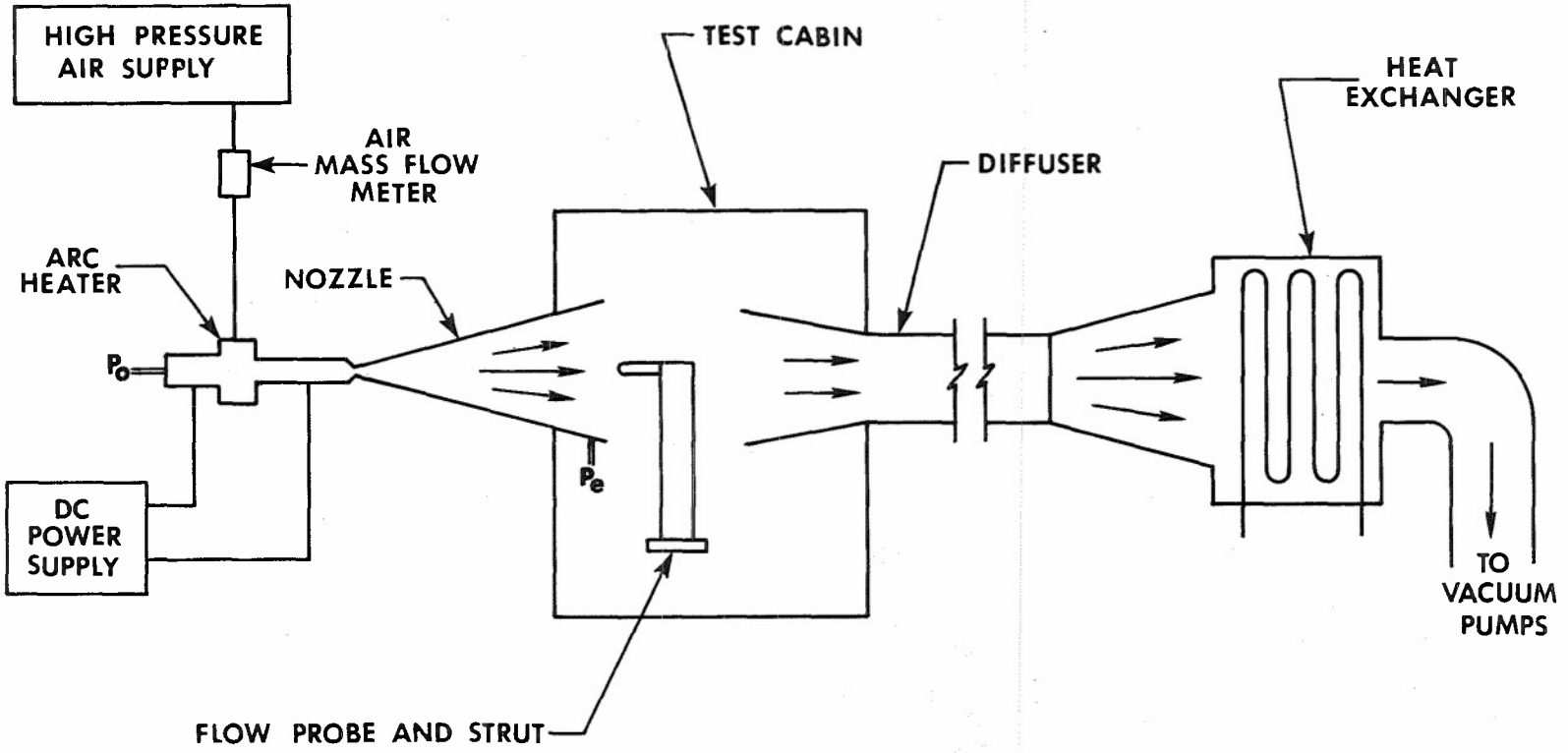

Figure 2. Schematic of Arc-Heated Wind Tunnel

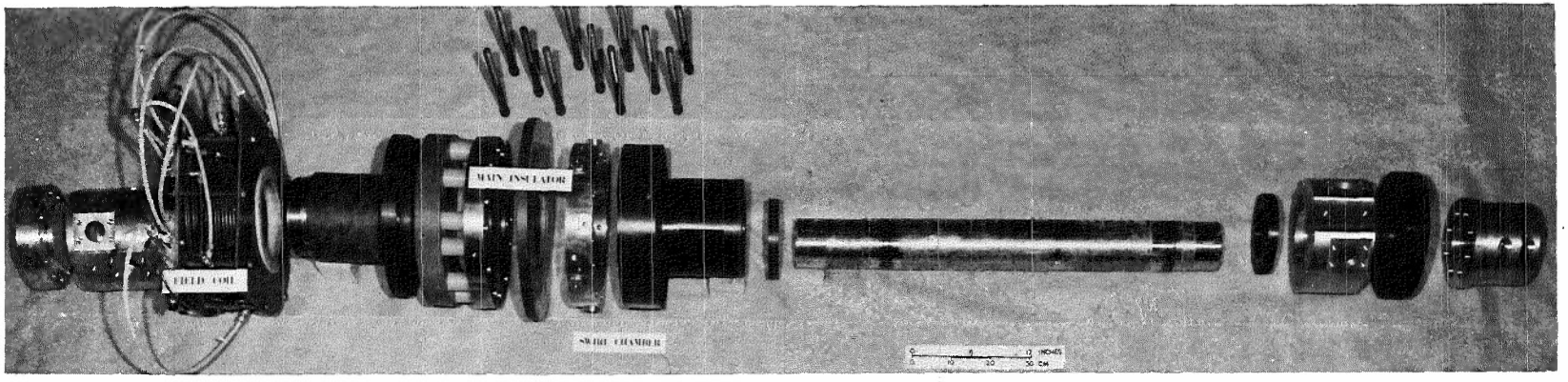

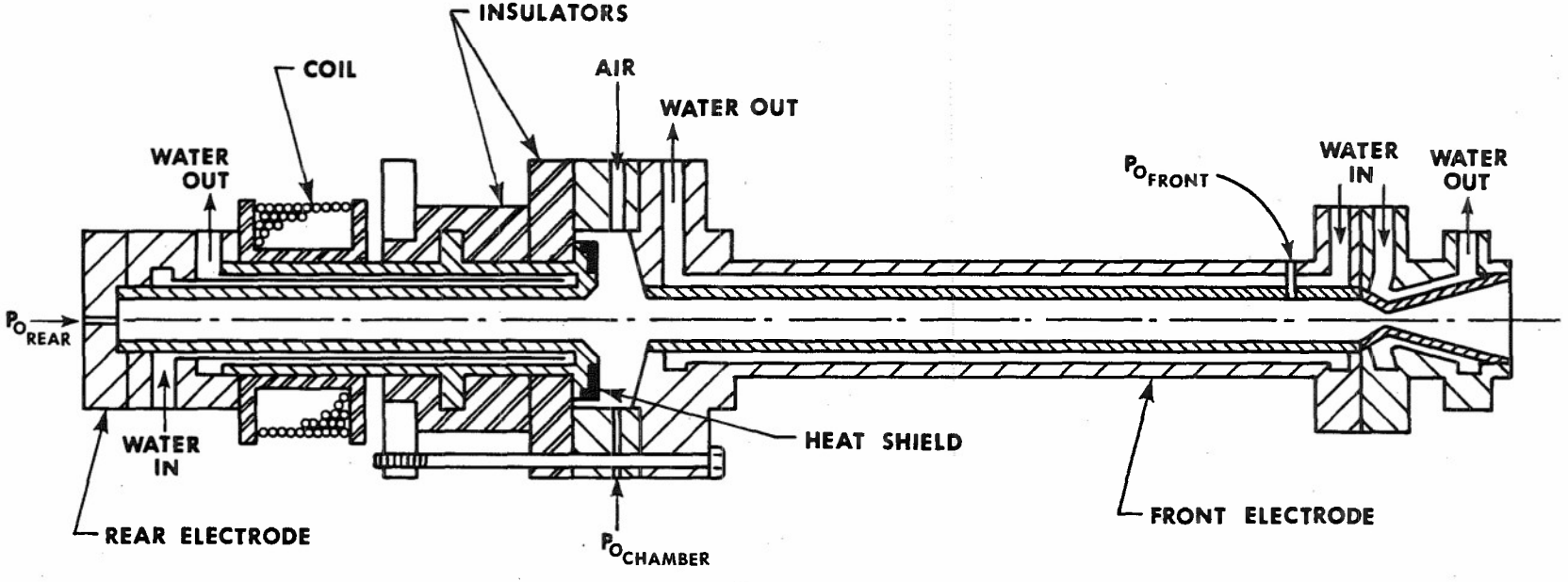

Figure 3. High Pressure Arc Heater

The arc heater, throat, and nozzle are cooled by circulating high pressure water in backside cooling channels. The water flow rates and the temperature rise of the cooling water are measured to determine the energy losses to the cooling system.

3. FLOW DIAGNOSTIC PROBES AND SUPPORT EQUIPMENT

The flow diagnostic probes used in this investigation consisted of a mass flux-total pressure probe, a small boundary layer pitot probe, and a stagnation point heat transfer probe shown in Figure 4. The detailed design aspects of the large flow probes are reported in Reference 12. The large probes were strut mounted and a photograph of the installation is shown in Figure 5. The coolant requirements for the strut and probes were supplied by a 20-channel cooling system specifically designed for supplying coolant to the various models and probes being tested.

a. Mass Flux-Pitot Pressure Probe

The mass flux probe is an aspirating type probe designed to fully capture a small stream tube of the free stream flow which is pumped through a calibrated orifice. The leading edge of the probe, is designed with a sharp lip inlet to achieve swallowing of the normal shock wave. Also incorporated into the probe design is a double bevel inlet lip to produce a locally symmetric flow field at the probe inlet. This type of configuration greatly reduces inaccuracies in determining the effective capture area which can occur with an asymmetric lip shape under the influence of strong viscous interactions. The local free stream mass flux (ρu) is obtained by dividing the measured mass flow rate by the probe inlet area:

$$\rho u = \dot{m} / A$$

To measure the pitot pressure a valve was installed in the probe aspirating flow line which stagnated the flow for the pitot pressure measurements. This method allowed for consecutive measurements leading to a more accurate flow calibration.

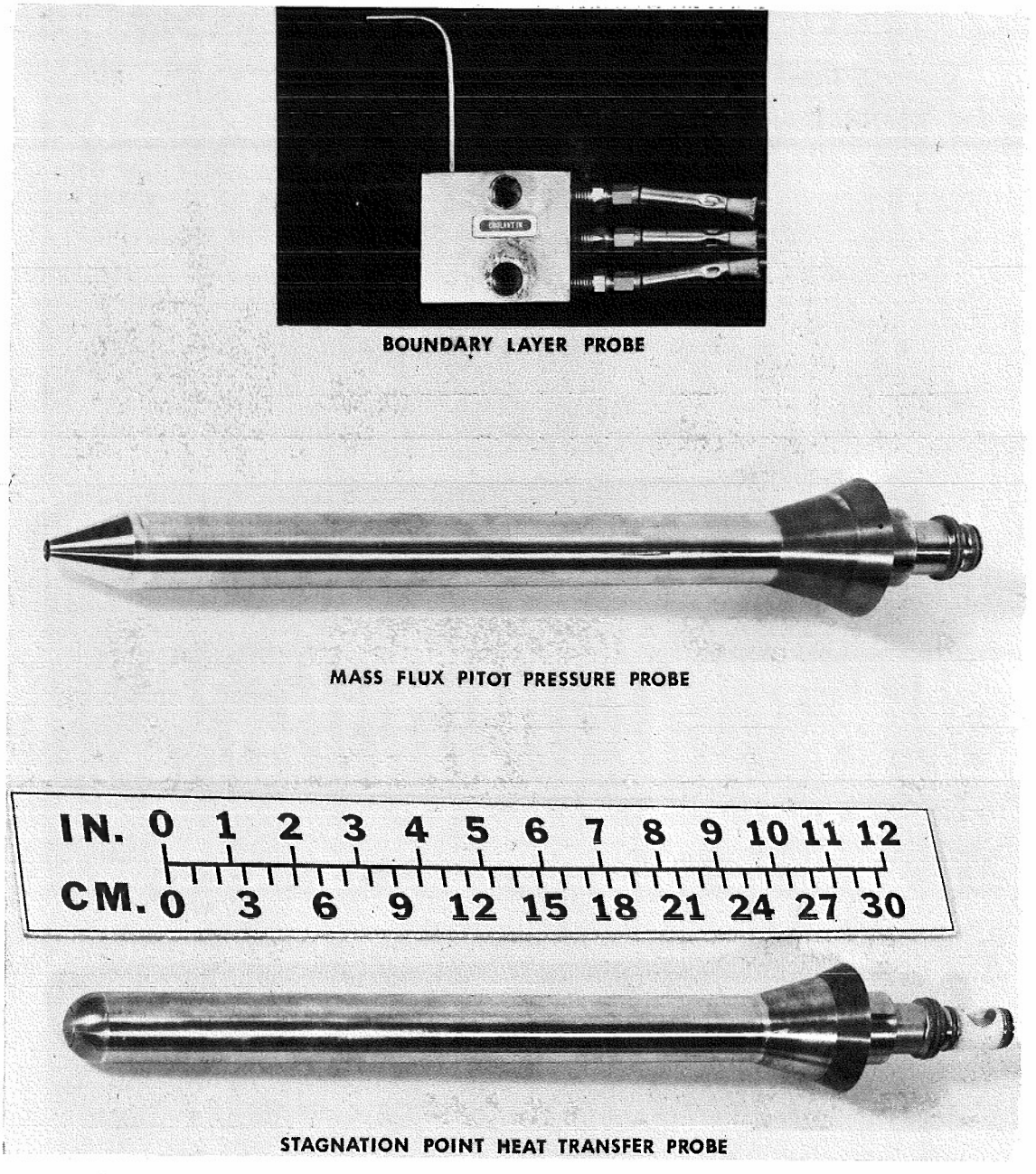

Figure 4. Flow Diagnostic Probes

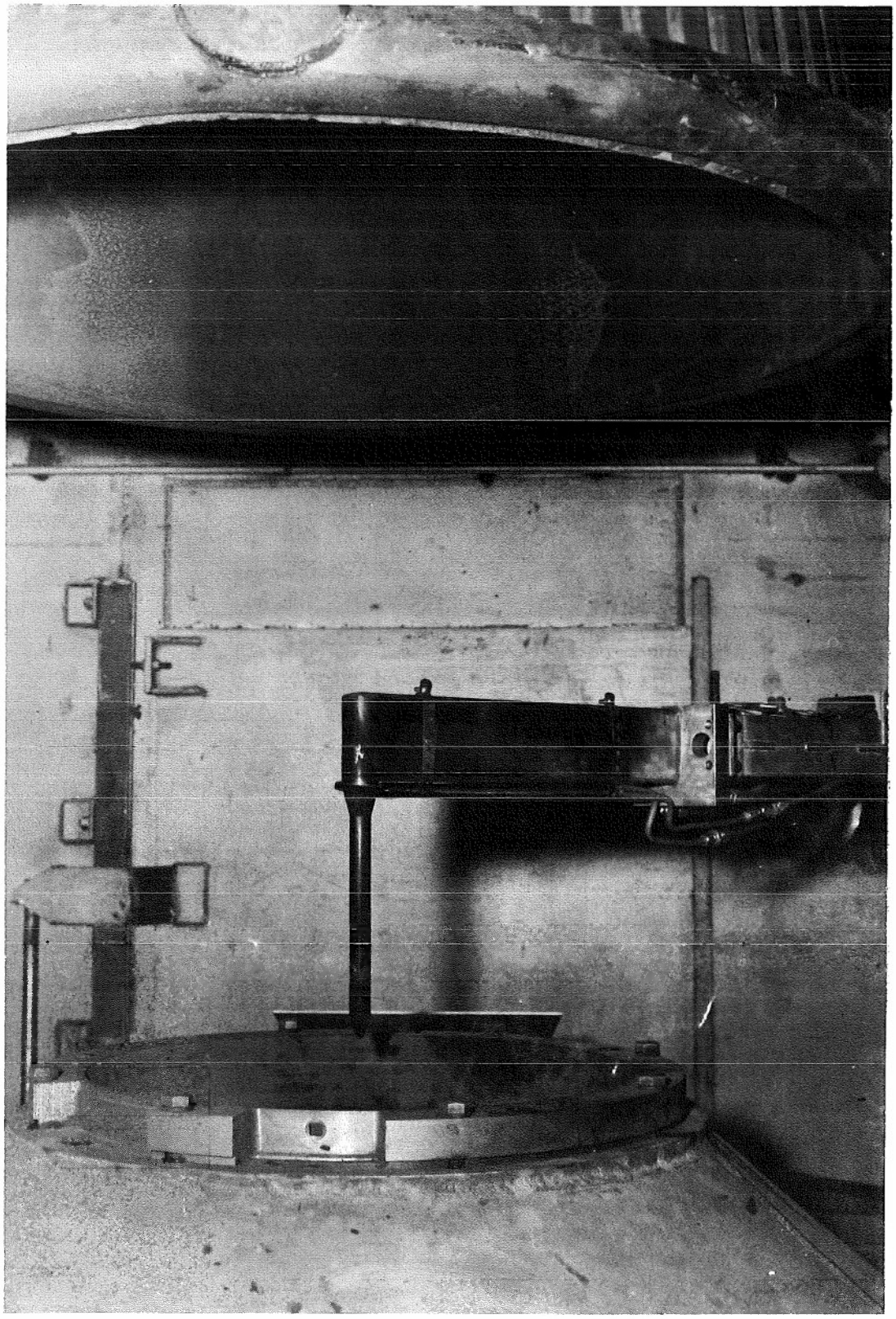

Figure 5. Mass Flux-Pitot Pressure Probe Installation

b. Stagnation Point Heat Transfer Probe

The heat transfer probe is a water cooled cylindrical probe with a hemispherical nose. The calorimeter section of the probe consists of a small thermally insulated copper slug located at the stagnation region of the nose. An integrated value of the heat transfer rate over the nose section is obtained by determining the heat input to this slug by measuring the temperature rise and flow rate of the cooling water. The stagnation point heat transfer rate is obtained by applying a small correction to the measured value to account for distribution effects.

The heat input to the nose cap ($\dot{Q}$) determined from the water flow rate and temperature rise is given by:

$$\dot{Q} = (\dot{m} C_p \Delta T)_{H_2O}$$

The ratio of the local heat transfer rate to the stagnation point heat transfer rate can be approximated for a hemispherical nose (Reference 13) by:

$$\dot{q}_\theta / \dot{q}_{sp} = \cos^{3/2}\theta$$

where θ is the angle between the free stream direction and local normal to the surface. The total heat input can also be determined by integrating the local heat transfer rate over the surface area:

$$\dot{Q} = \int \dot{q}_\theta \, dS = 2\pi R^2 \dot{q}_{sp} \int \cos^{3/2}\theta \sin\theta \, d\theta$$

which can then be integrated to give:

$$\dot{q}_{sp} = \frac{\dot{Q}}{0.8\pi R^2 \left[1 - \cos^{5/2}\theta\right]}$$

4. DATA ACQUISITION SYSTEMS

The primary data acquisition equipment for these tests consisted of an Ambilog hybrid (analog-digital) data processor. Analog data signals from the tunnel instrumentation are processed through signal conditioning equipment, fed into the processor, computed, and then stored in digital form on magnetic

tape. Run identification and a time reference are also recorded with each data scan. All the programmed data channels were recorded for each test point at a rate of 16 samples per second for a time interval of from 2 to 10 seconds. Immediately at the conclusion of each run, the individual data points are time averged using selected time intervals for each.

SECTION III
EXPERIMENTAL PROCEDURE AND DATA PRESENTATION

1. GENERAL TEST PROCEDURE

Prior to arc heater firing, the tunnel circuit including the arc heater was evacuated to a pressure of approximately 10 mm Hg. The arc heater was then started by closing the master power breaker imposing open circuit voltage across the electrodes. Sensing of the current as the arc was initiated automatically opened the air supply valve and the heater quickly established the preset starting conditions. The arc voltage and current were then adjusted to give the desired test conditions. Once the flow was established, the diffuser jet pumping action further evacuated the test cabin giving an overexpanded free jet. Steady state conditions were obtained in less than 30 seconds.

The probe was then inserted into the flow and positioned radially across the jet by manual control of the hydraulic drive control system. Longitudinal positioning of the probe was accomplished prior to the run and was located a minimum of one inch downstream of the nozzle exit plane to insure clearance during insertion. The surveys were made using a step-pause technique to eliminate the possibility of errors caused by slow time response instrumentation.

During the surveys, the measured parameters and the probe positions were recorded on X-Y plotters and displayed from the computer to assist the operator in positioning the probes and to determine when the parameters had reached a steady-state value. At each test point the data acquisition system was activated and all data channels, including the arc heater parameters, were simultaneously recorded, computed, and stored on magnetic tape. Several test conditions could be obtained during a run by resetting the arc heater conditions and repeating the test sequence. Typical continuous run duration for this test series was from 10 to 30 minutes. During the test, periodic instrument checks and calibrations insured the accuracy of the measured value of the various parameters.

2. ARC HEATER PERFORMANCE

These flow studies were conducted in conjunction with an extensive arc heater development program which is reported in Reference 11; a typical performance curve is presented in Figure 6. The initial runs were made with a 45-inch long front electrode installed in the heater. For this electrode length, the arc would blow through the throat and terminate downstream on the nozzle wall when the arc chamber pressure exceeded approximately 500 psi. This caused a highly ionized core at the flow center line. To alleviate this condition, the electrode length was increased to 72 inches and finally to 96 inches. The increased length permitted heater operation at successively higher reservoir pressures and improved the flow uniformity at the nozzle exit. The heater efficiency dropped slightly but generally ranged from 35 to 60% for all the operating conditions and configurations tested. The majority of the test program was accomplished using a one-inch diameter throat which operated at reservoir pressures from 300 to 1500 psi and input power to 35 megawatts. Using a two-inch diameter throat restricted the pressure range from 100 to 500 psi but permitted operation at higher enthalpy levels with input powers to 51.7 megawatts. Bulk or heat balance enthalpies ranging from 1500 BTU/lb to 4000 BTU/lb were obtained.

3. NOZZLE EXIT MEASUREMENTS

Nozzle exit surveys and center line measurements of the pitot pressure, mass flux, stagnation point heat transfer rate, and wall static pressure were

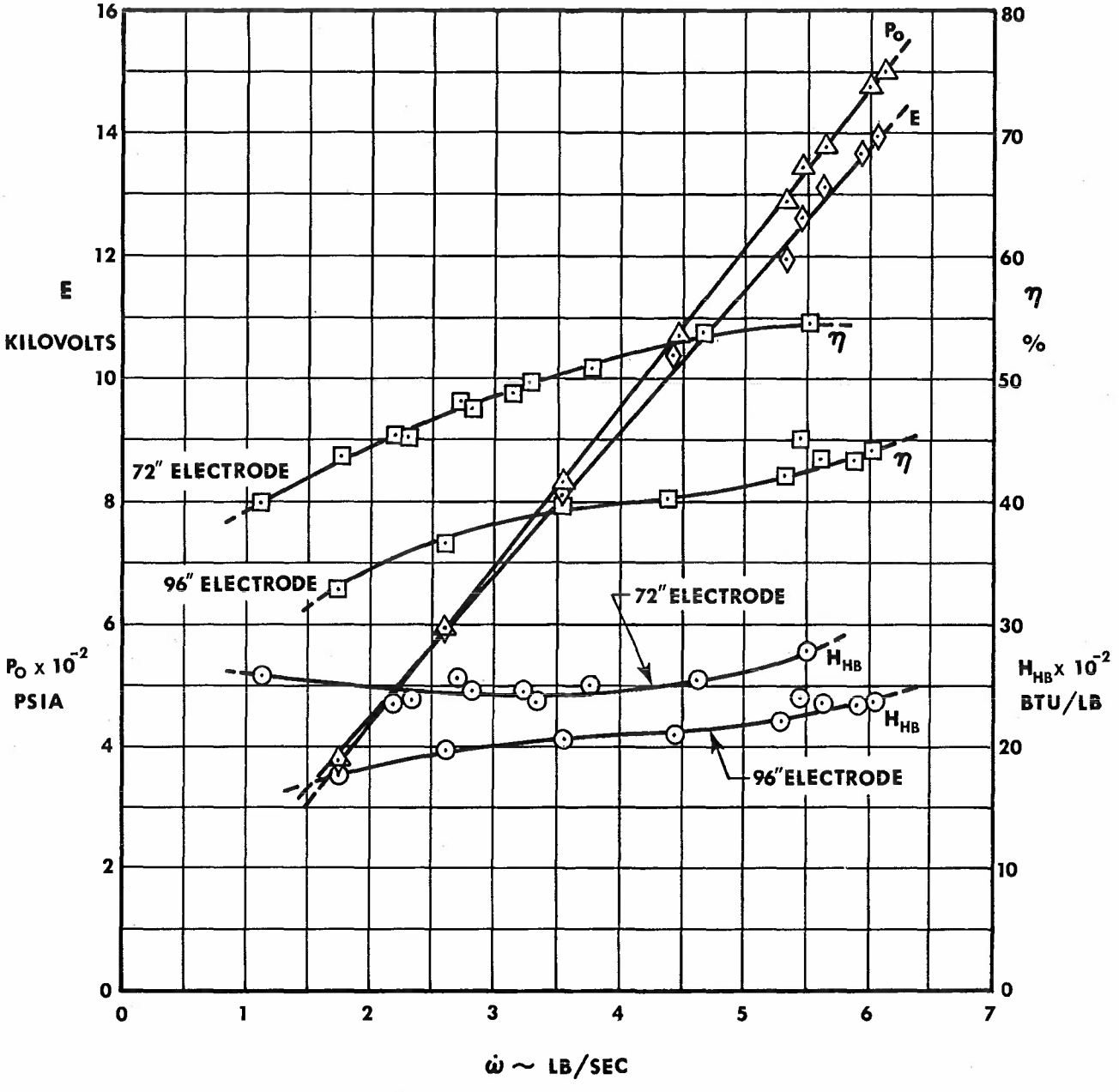

Figure 6. Typical Arc Heater Performance Characteristics ($d^* = 1.0$, $I = 2400$)

obtained for all available reservoir conditions. The center line pitot pressure measurement and wall static pressure data are discussed in Section IV.3. The radial flow surveys made during these tests were of major importance in the flow field calibration. These surveys have shown that arc heater configuration, particularly the front electrode length, exhibited a strong influence on the nozzle exit flow uniformity.

a. Pitot Pressure-Mass Flux Surveys

Radial P_{T_2} and ρu profiles were flat within 5% for all the arc heater configurations and reservoir conditions tested. Pitot pressure and mass flux surveys made with the 72-inch and 96-inch electrode configurations are shown in Figures 7 through 10. From these figures it can be noted that, for the short electrode lengths, as the reservoir pressure is increased the profiles dipped slightly on the center line. The same effects can also be noted in Figure 11 which shows typical surveys with the 45-inch electrode at high arc current operation. Subsequent tests showed that these surveys alone can give a misleading picture of the uniformity of the flow field.

Detailed pitot pressure profiles in the boundary layer were obtained for several operating conditions and are shown in Figure 12. The small water cooled pitot probe was used for the measurements near the wall to improve the resolution and positioning accuracy.

Flow profiles of the ratio of pitot pressure to stagnation pressure have been calculated for expansion area ratios (A/A*) of 156 and 625. These data presented in this form in Figures 13 and 14 show that the profiles are relatively independent of other operating parameters and reduce to a single curve. Profiles of the ratio of the free stream to local mass flux, given in Figure 15, show that this parameter is also independent of pressure.

b. Stagnation Point Heat Transfer Data

Stagnation point heat transfer rate profiles and center line measurements were made for numerous arc heater operating conditions. On the first few runs made with the probe it was noted that a black copper oxide coating would

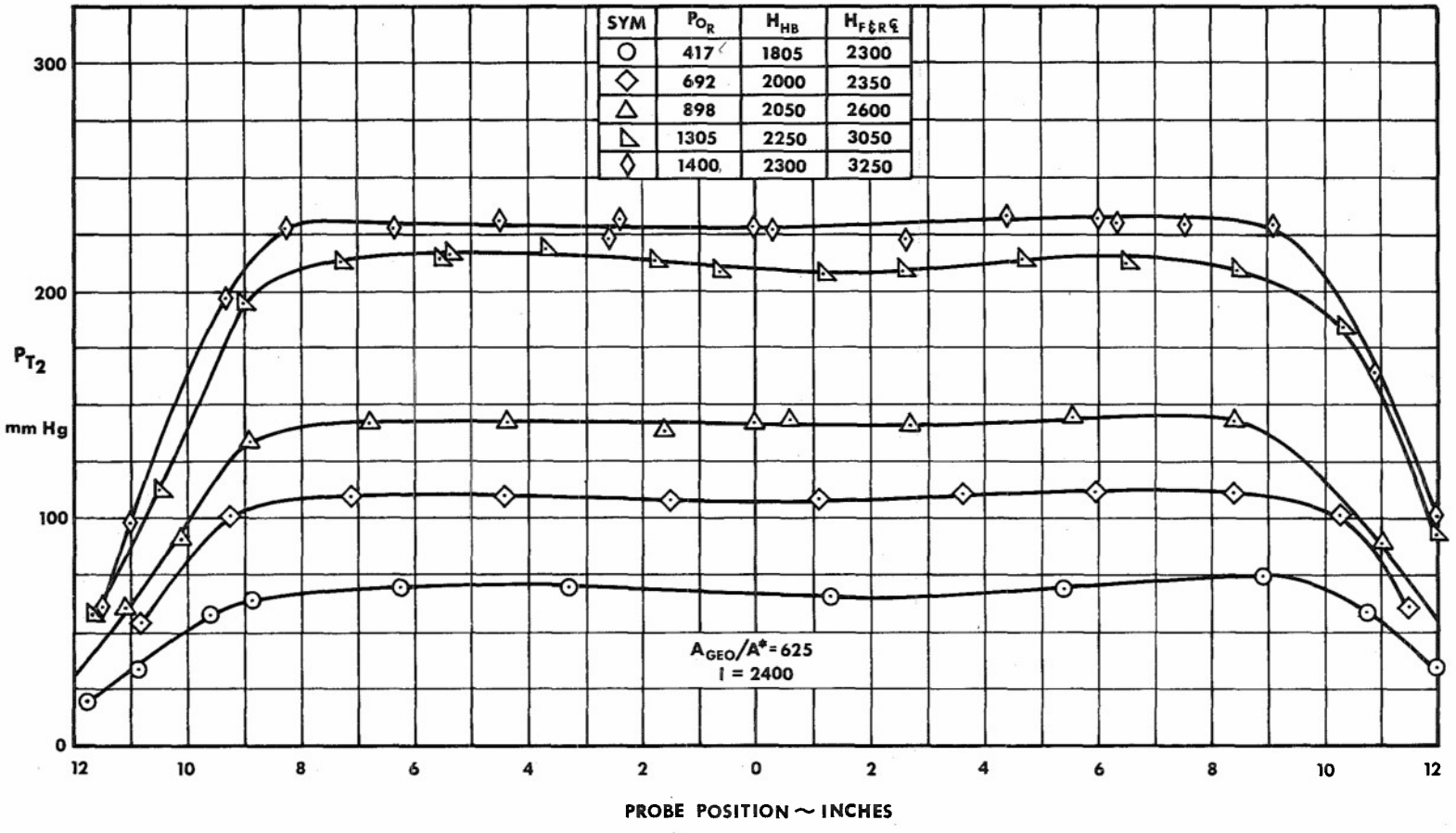

Figure 7. Typical Pitot Pressure Profiles, With 96" Electrode

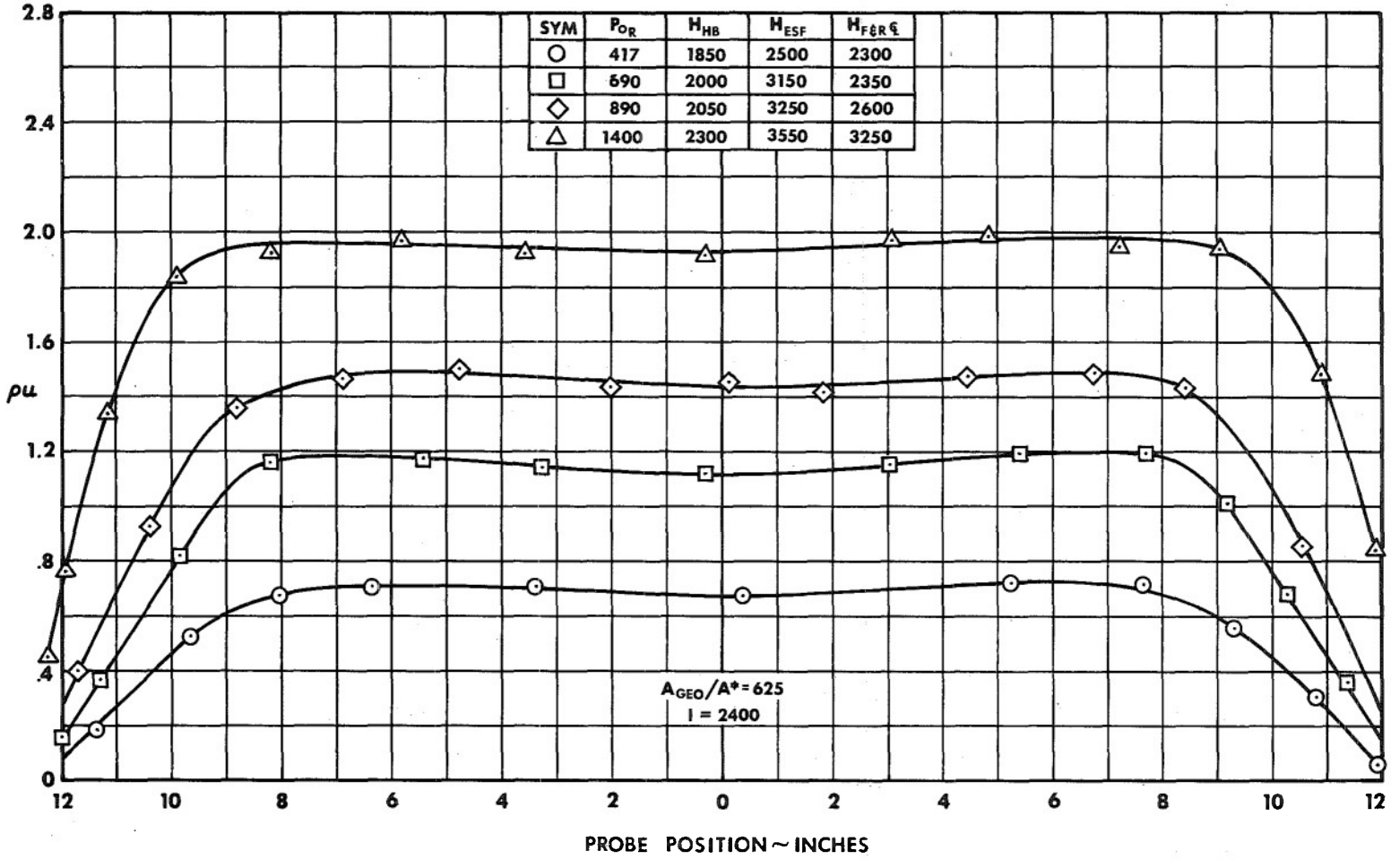

Figure 8. Mass Flux Profiles, With 96" Electrode

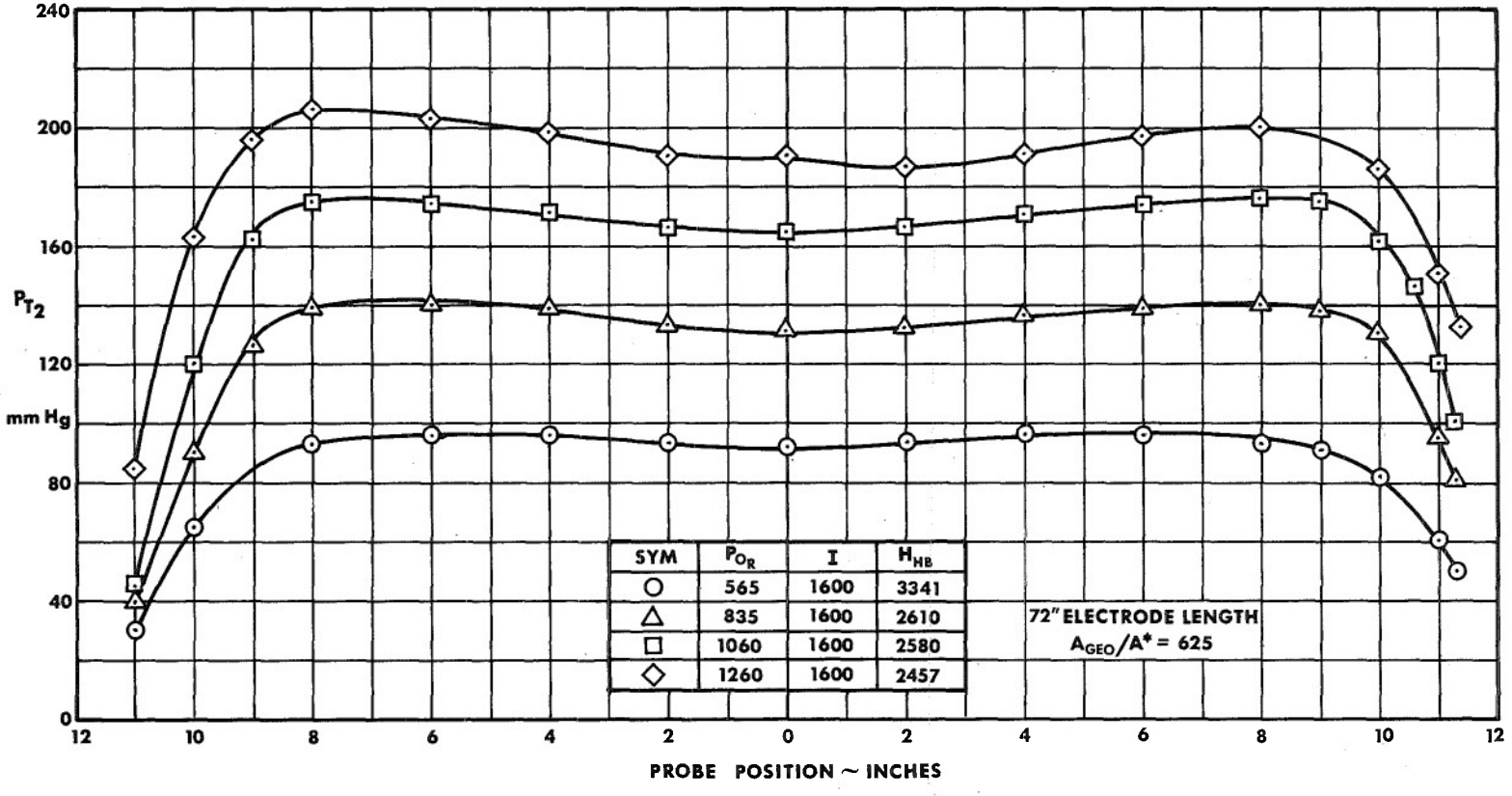

Figure 9. Typical Pitot Pressure Profiles, With 72" Electrode

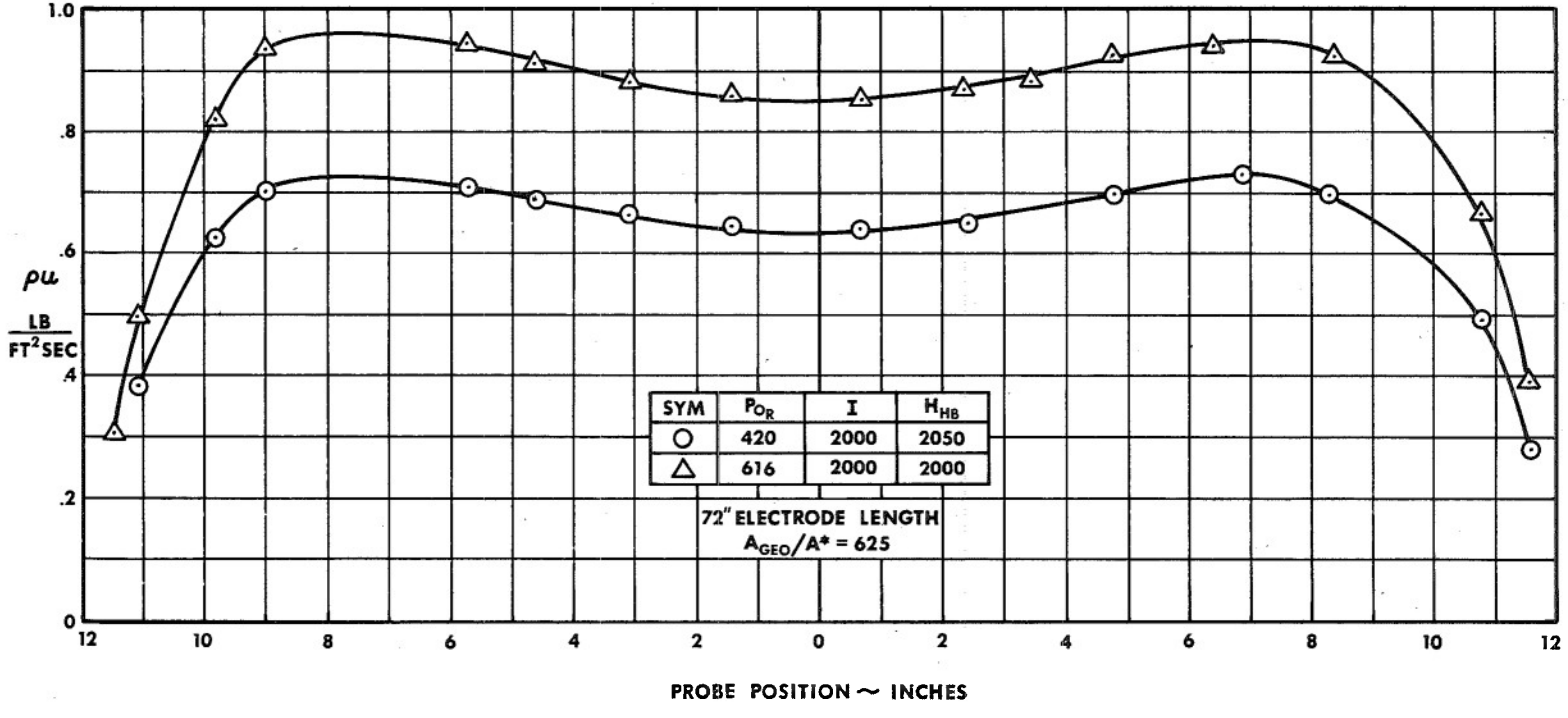

Figure 10. Mass Flux Profiles, With 72" Electrode

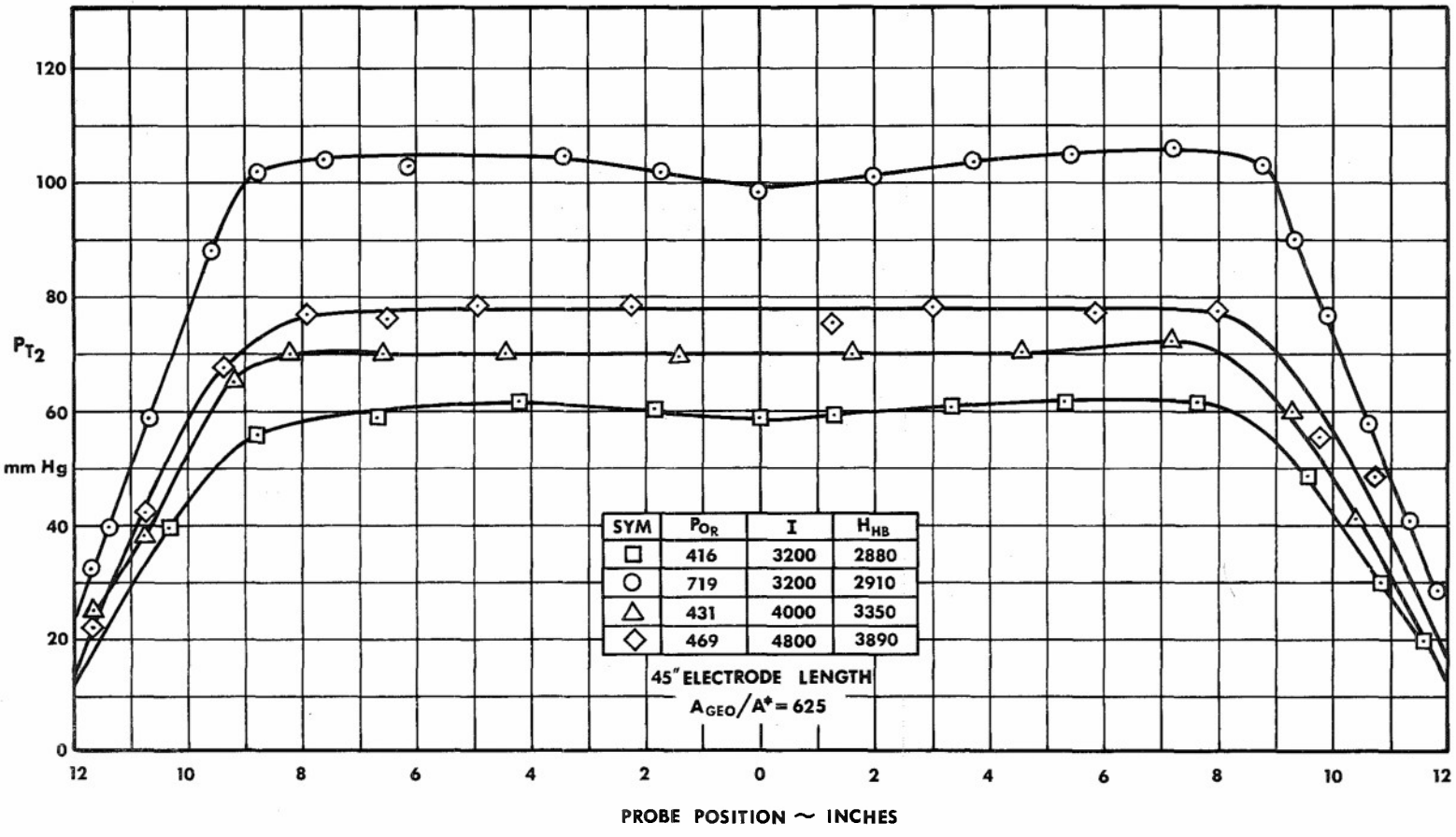

Figure 11. Typical Pitot Pressure Profiles at High Operating Currents, With 45" Electrode

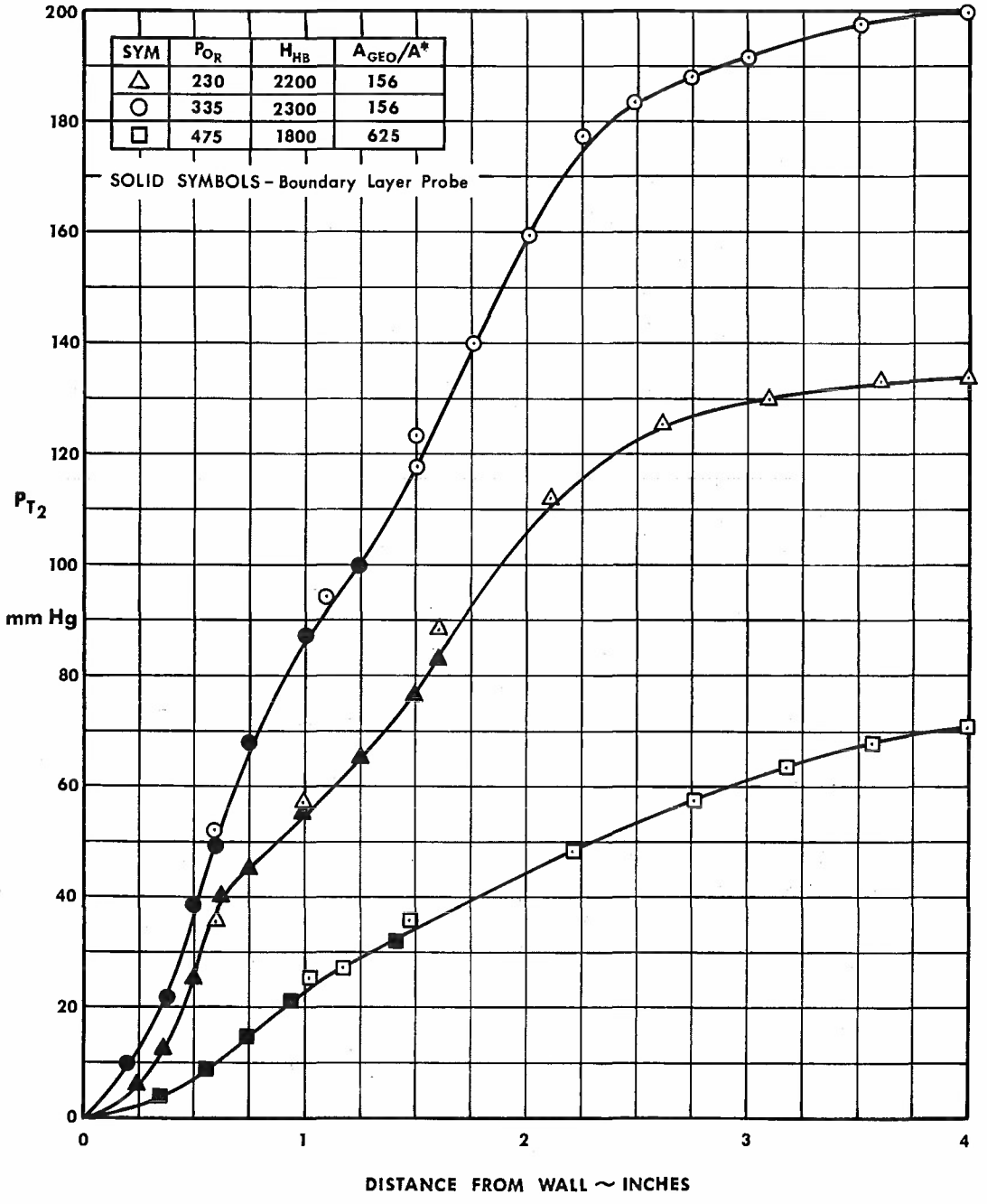

Figure 12. Boundary Layer Pitot Pressure Profiles

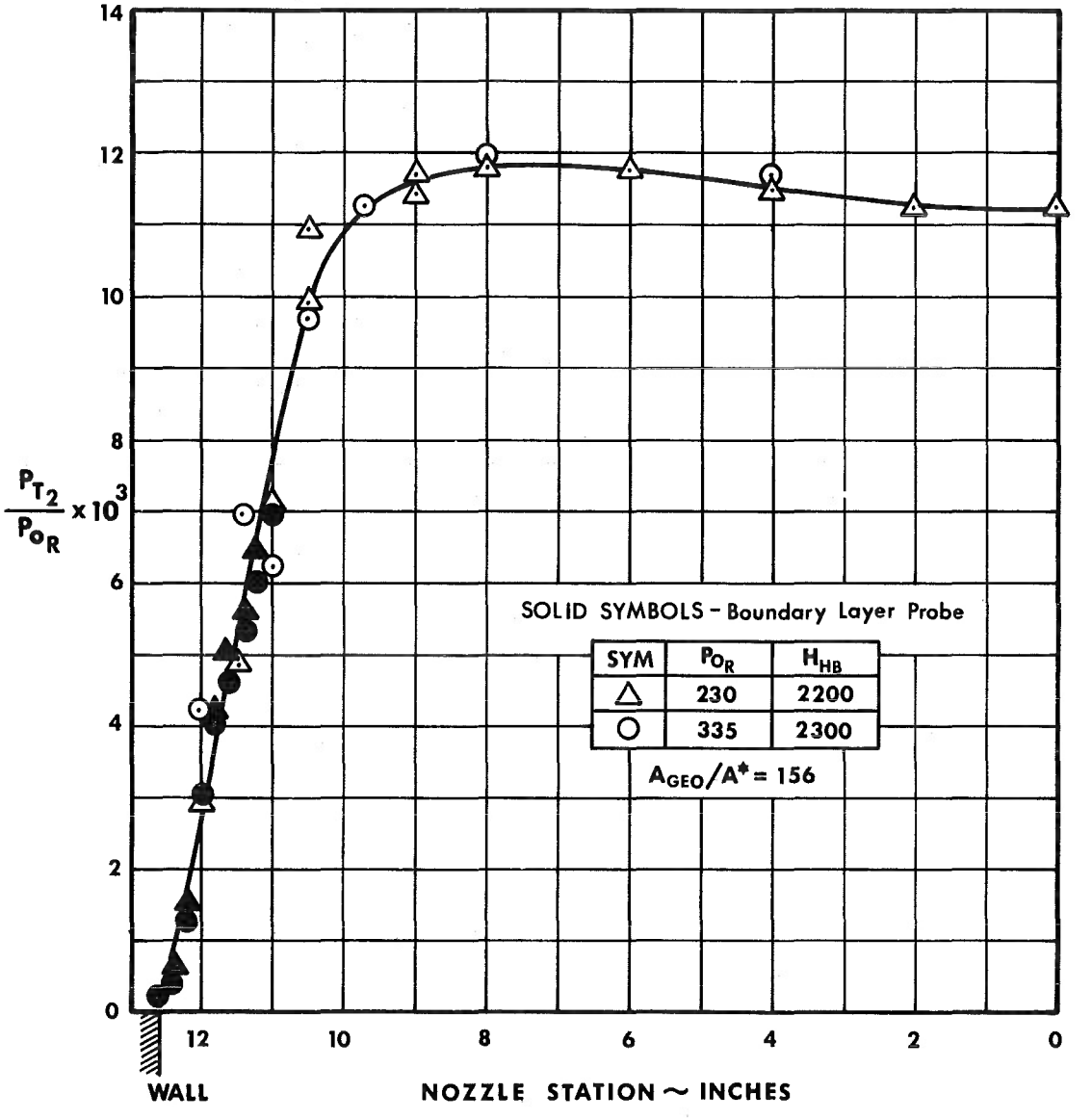

Figure 13. Non-Dimensionalized Pitot Pressure Survey, A/A* = 156

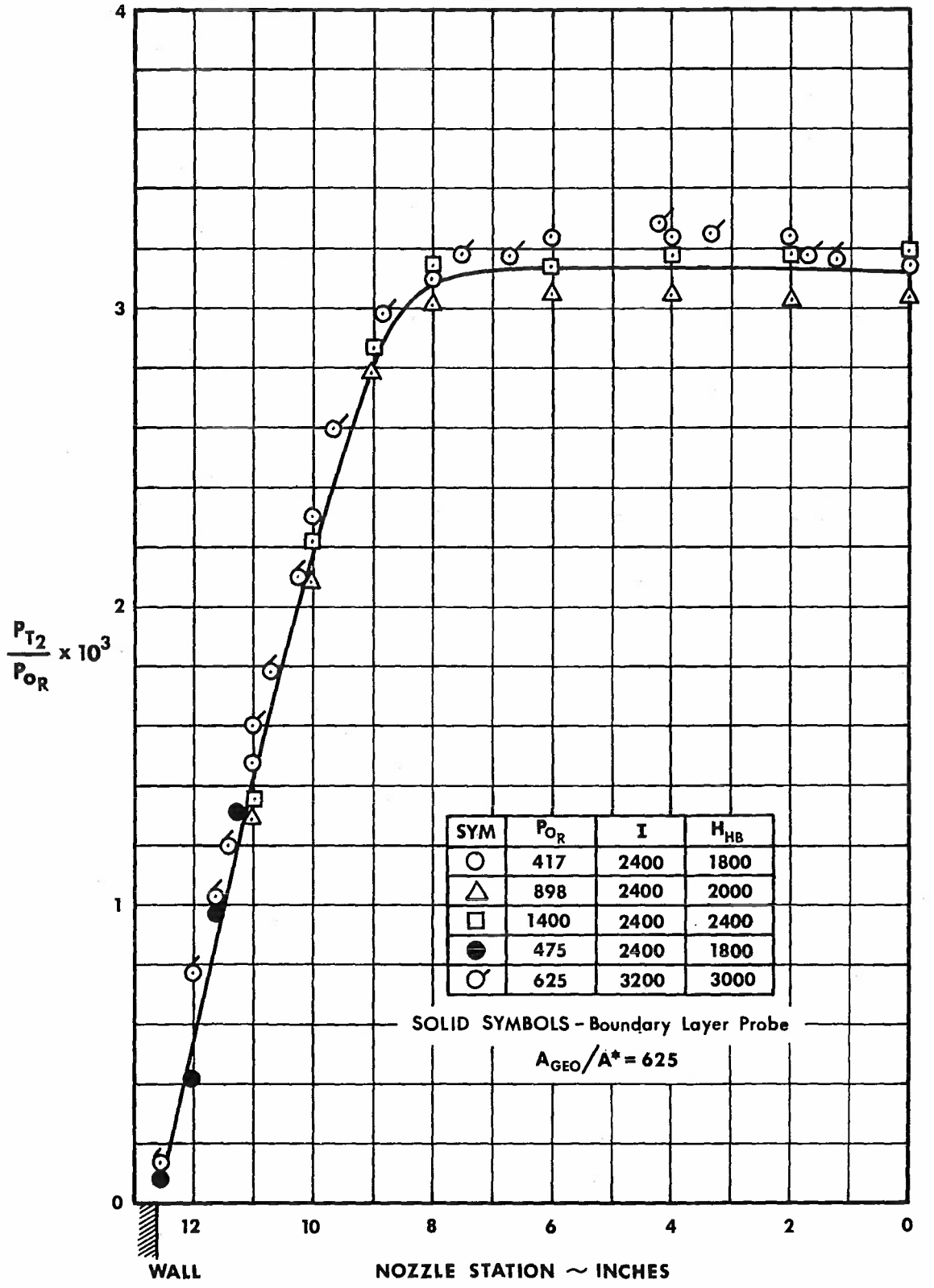

Figure 14. Nondimensionalized Pitot Pressure Profile, A/A*= 625

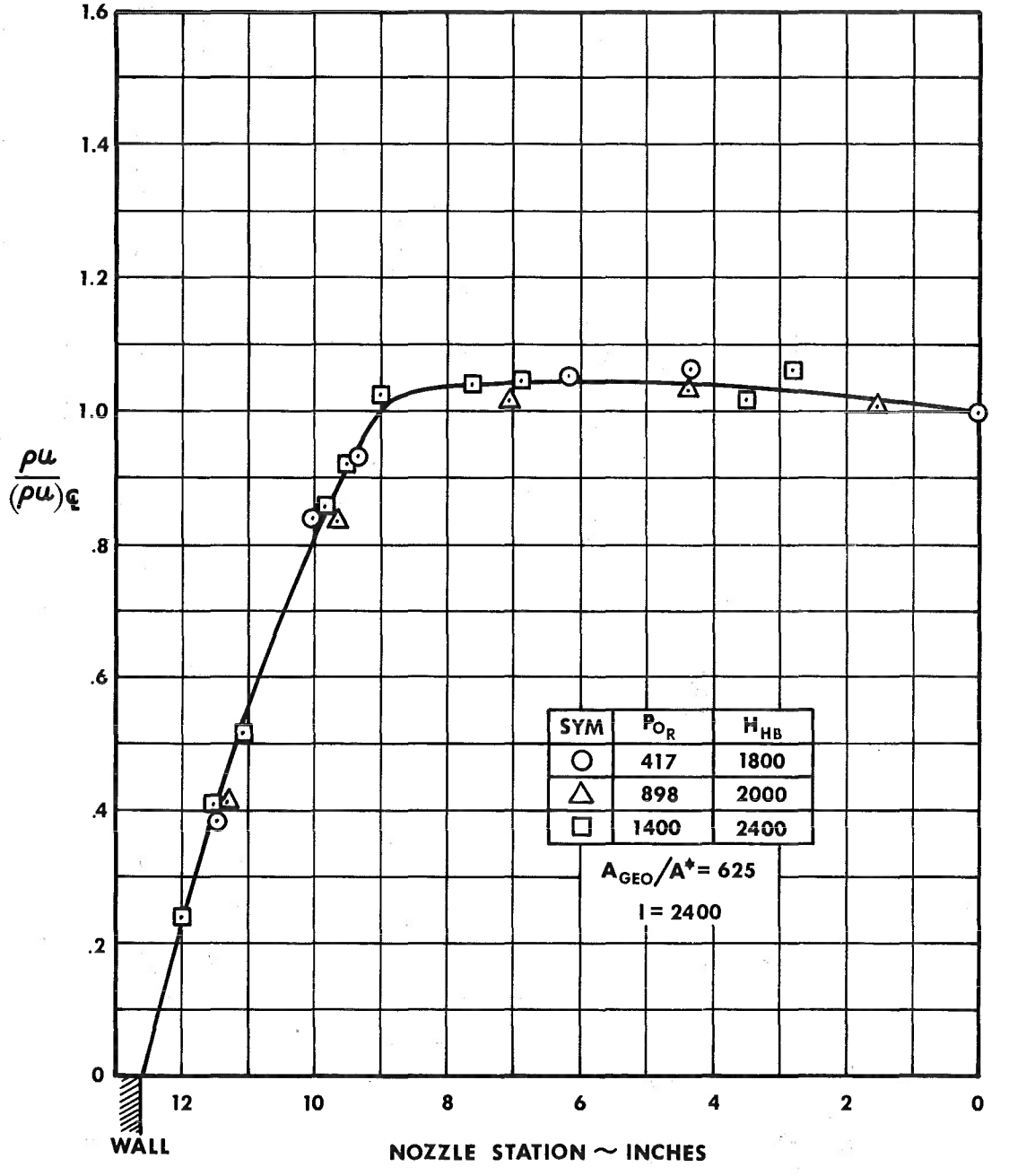

Figure 15. Nondimensionalized Mass Flux Profile

form over the copper sensing slug as well as remaining probe surfaces. The work of Goulard (Reference 14) has shown that surface materials of this type can make the wall noncatalytic to atom recombination and cause a significant reduction of the heat transfer rate. Several runs were made to investigate the effects of the oxide formation on the heating rate. Prior to these runs the copper sensing slug was polished and gold plated to insure a highly catalytic surface. The probe was inserted into the flow at steady-state conditions for extended periods of time and the heating rate was monitored as the oxide layer formed. There was no measurable reduction of the heat transfer rate and therefore it was concluded that these measurements could be used in conjunction with equilibrium heating rate theory to determine the total enthalpy of the flow.

Initially, the center line measurements of the heat transfer rate shown in Figures 16 and 17 were difficult to interpret due to the wide data scatter and inconsistent trends. These data were brought into proper perspective by examining the complete radial profiles at various operating conditions. The effects of heater pressure on the profile shape for the 72- and 96-inch electrode configurations are shown in Figures 18 and 19. Note that with the short front electrode the profiles peaked at much lower pressures and that the arc heater with long electrodes could be operated at pressures in excess of 1000 psi with uniform profiles across the core. The effect of arc current is shown in Figure 20. These runs were made at approximately the same pressure and show that increasing the current shortens the arc and thus decreases the peaking. However, profiles given in Figure 21 show that very high arc currents will cause the peaking phenomenon even at low operating pressures.

4. TOTAL ENTHALPY MEASUREMENTS

The total enthalpy of the gas is one of the most important test parameters to be duplicated and therefore several methods of measuring it were employed.

a. Heat Balance Method

An energy balance of the arc heater and nozzle can be made by measuring the electric power input to the heater and the energy loss to the cooling water. The DC power to the arc heater was determined by continuously monitoring

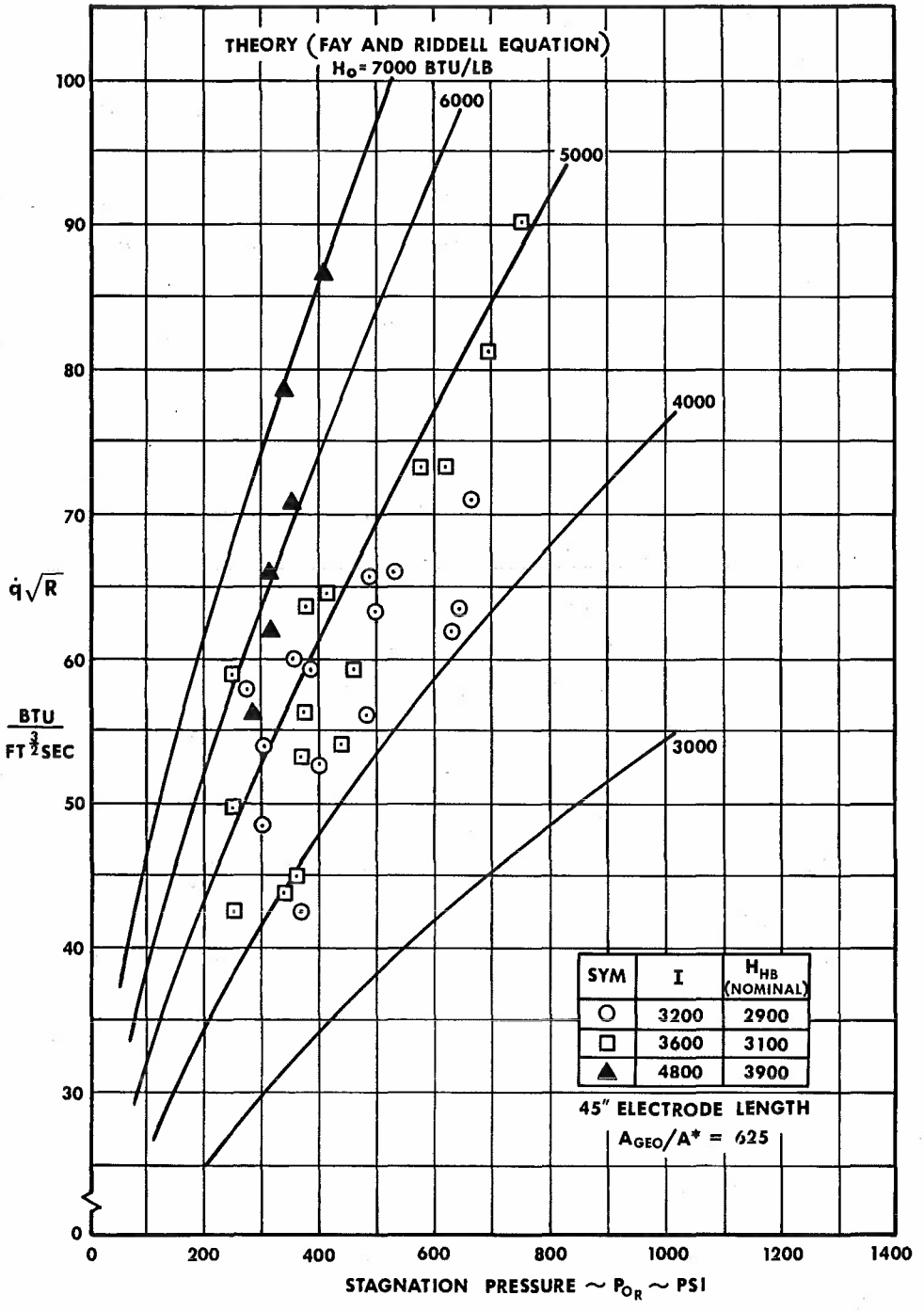

Figure 16. Typical Center Line Stagnation Point Heat Transfer Rate Measurements, With 45" Electrode

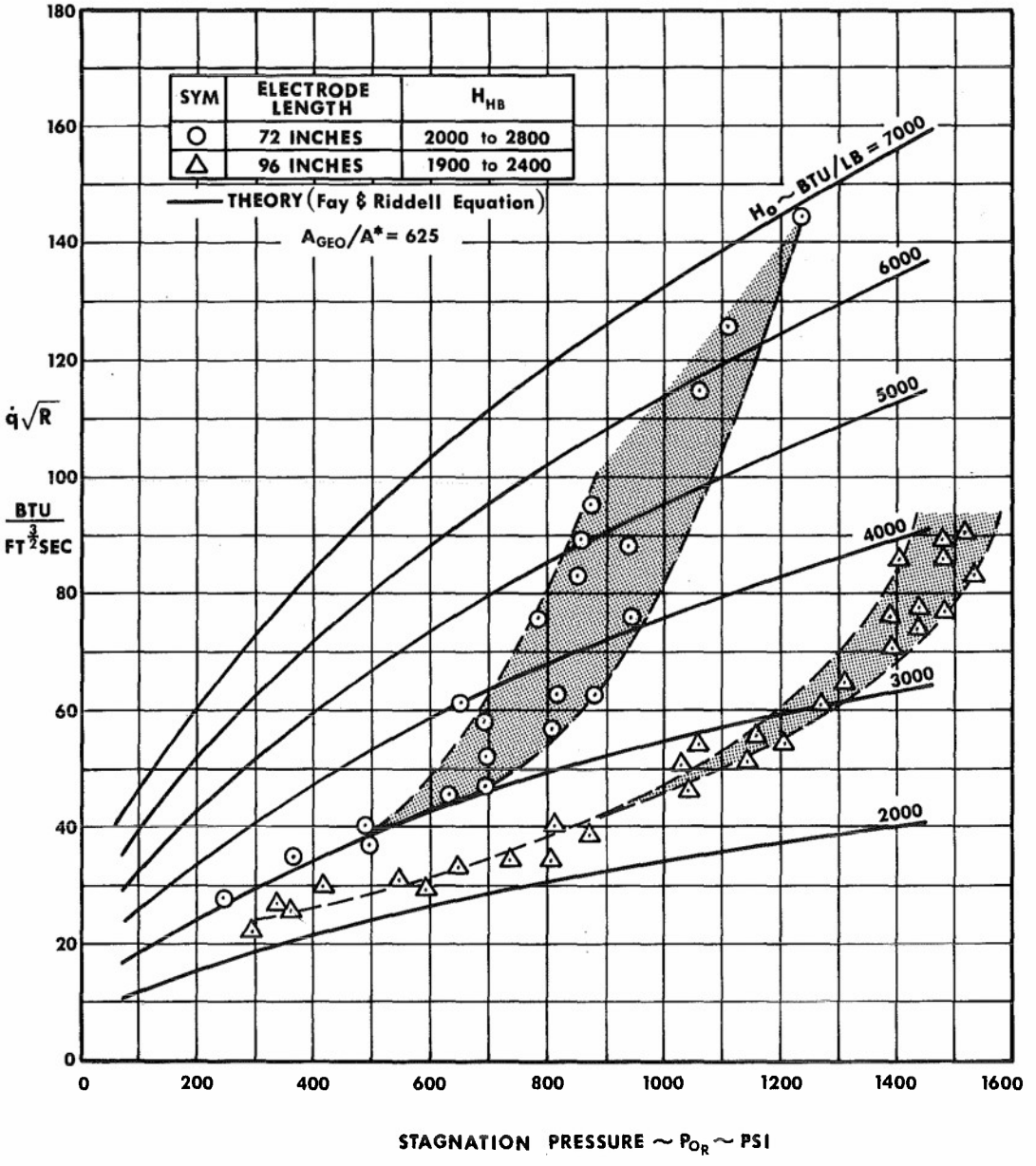

Figure 17. Typical Center Line Stagnation Point Heat Transfer Rate Measurements With 72" and 96" Electrodes (I = 2400)

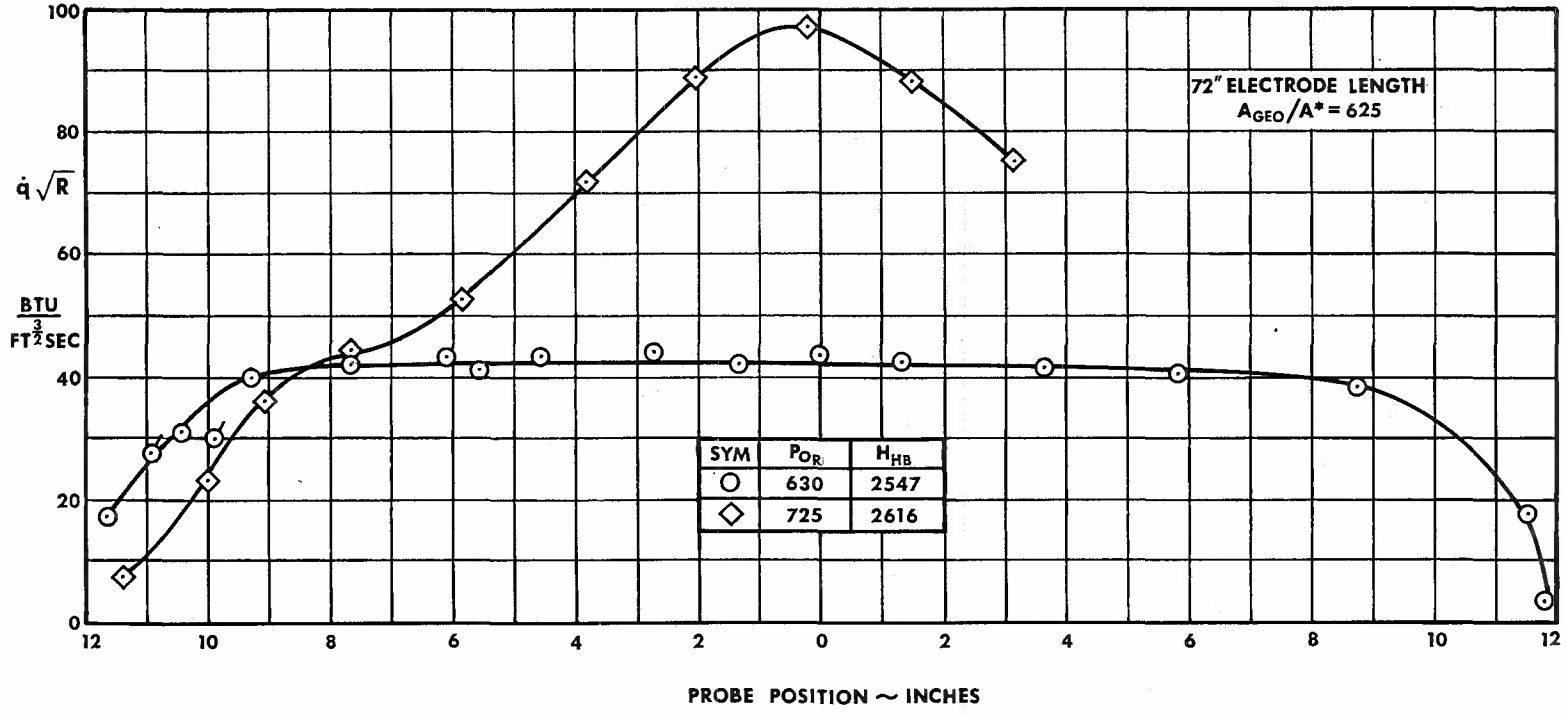

Figure 18. Stagnation Point Heat Transfer Rate Profiles Showing the Effects of Pressure on Flow Uniformity, With 72" Electrode

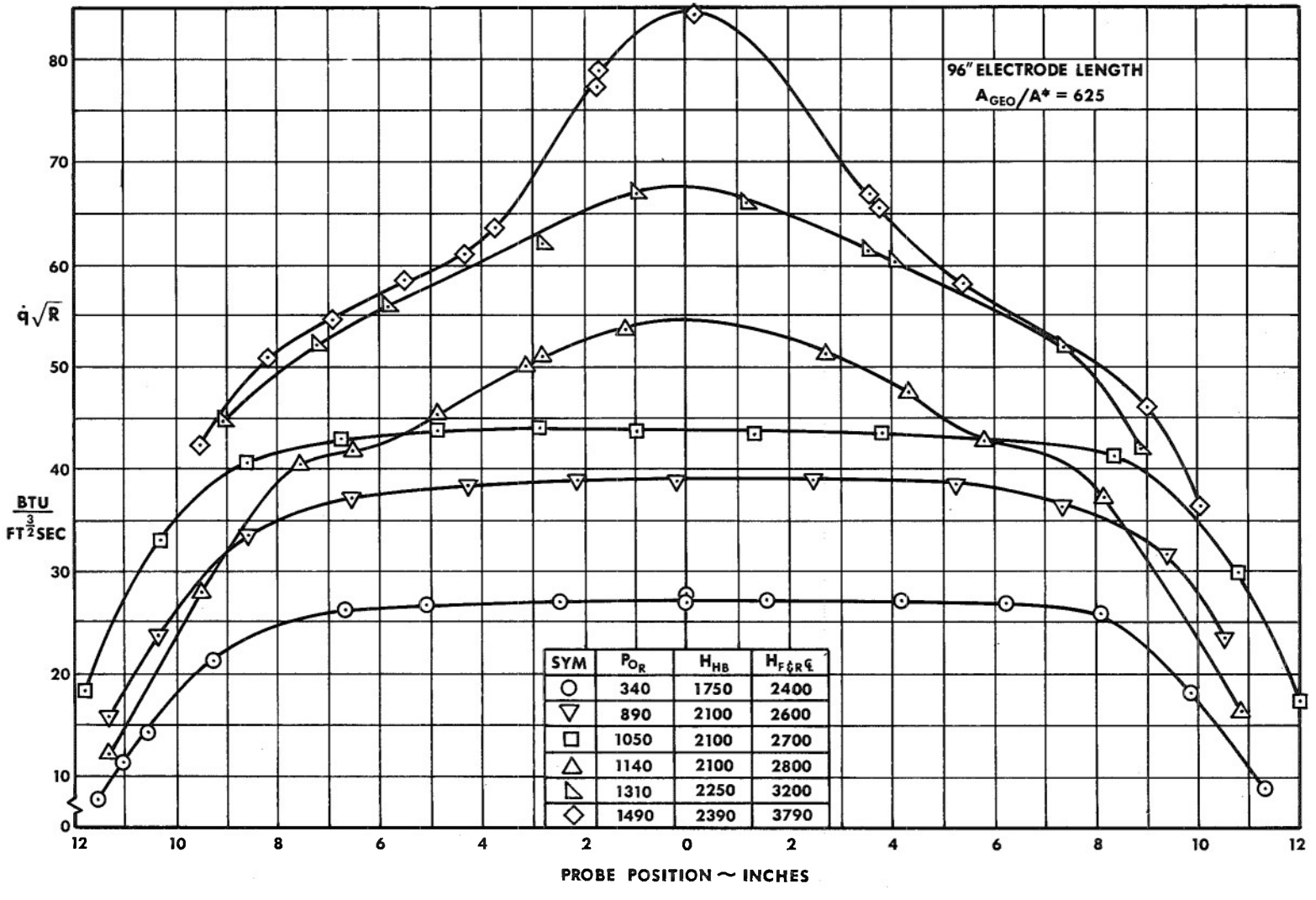

Figure 19. Stagnation Point Heat Transfer Rate Profiles Showing the Effect of Pressure on Flow Uniformity, With 96" Electrode

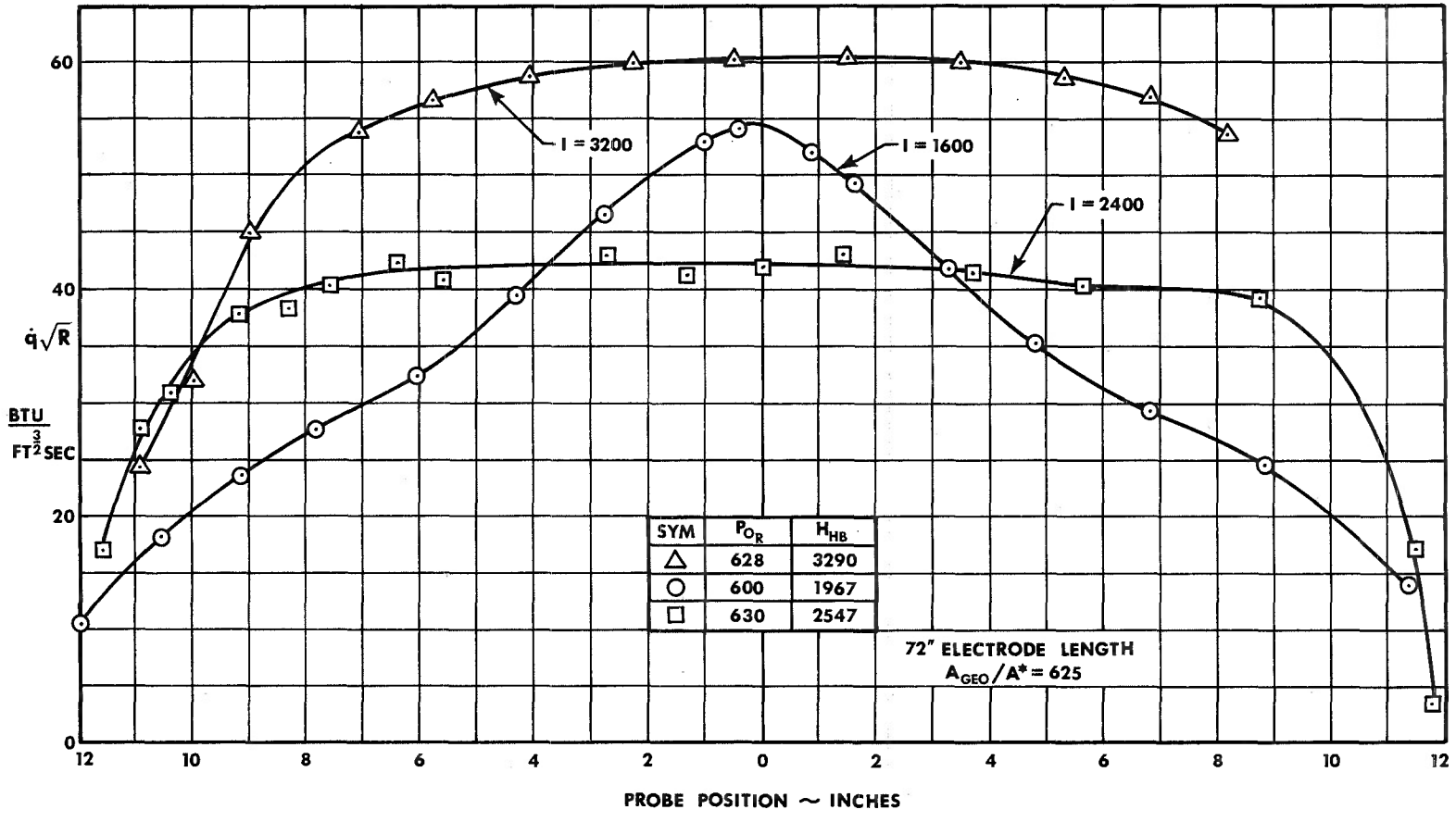

Figure 20. Stagnation Point Heat Transfer Rate Profiles Showing the Effect of Current on Flow Uniformity, With 72" Electrode

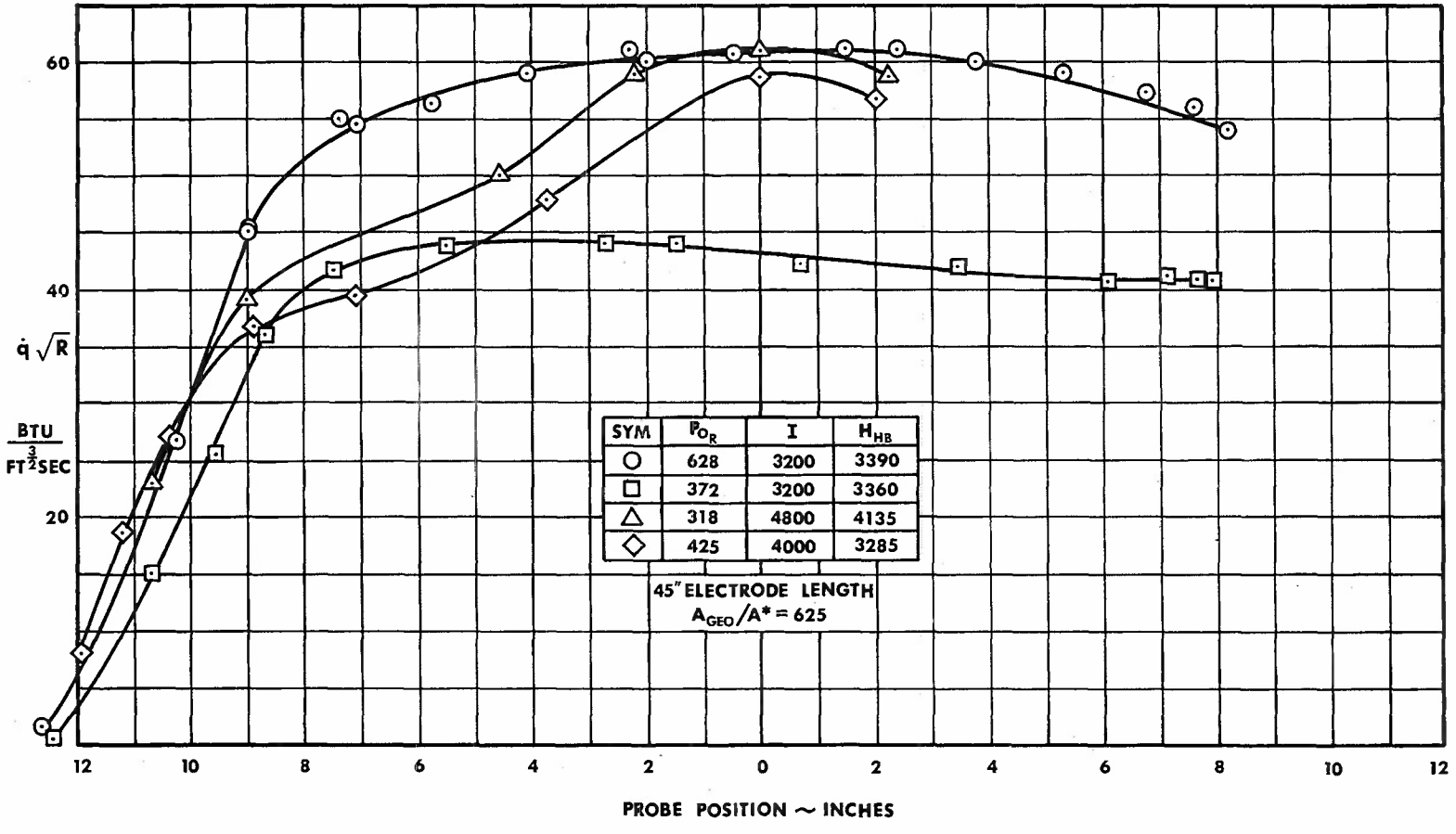

Figure 21. Stagnation Point Heat Transfer Rate Profiles at High Operating Currents, With 45" Electrode

the operating voltage and current. The air mass flow rate was measured with an unchoked calibrated orifice located upstream of the heater. The cooling water flow rates to the electrodes and swirl chamber, and the temperature rise of the water were used to determine the energy loss in the heater, from which the heater efficiency and heat balance enthalpy were calculated. The losses to the throat were a maximum of 2.5% of the heater input power and were not included in the heat balance enthalpy calculations. Combining the heater energy balance with the air flow rate gives the bulk or heat balance enthalpy:

$$H_{HB} = \left[EI - (\dot{m} C_p \Delta T)_{H_2O} \right] / \dot{\omega}$$

The heat balance enthalpy being a bulk measurement is not representative of the true center line enthalpy because of the nozzle boundary layer and the incomplete heat diffusion from the arc.

b. Equilibrium Sonic Flow Method

The total enthalpy of the flow can also be obtained from the throat area, air mass flow rate, and stagnation pressure by using the equilibrium sonic flow theory. An empirical expression of this type formulated by Winovich (Reference 15) is given by:

$$H_{esf} = \left(\frac{280 A^* P_o}{\dot{\omega}} \right)^{2.519}$$

The assumption inherent in this equation is that the flow can be represented by a uniform one-dimensional equilibrium flow through the throat with a discharge coefficient of one. The arc heater geometry and flow pattern and gas chemistry must be critically analyzed to determine the applicability in each particular case.

The equilibrium sonic flow enthalpy was calculated for the present test conditions and compared with the enthalpy based on the heat transfer probe and the heat balance enthalpy. This comparison shows that the sonic flow enthalpy calculated from the above equation was as much as 30% higher than

the center line heat transfer probe enthalpy and approximately 50% higher than the heat balance enthalpy. The higher enthalpy is believed to be caused by the reduction of the effective throat area due to a strong swirl flow in the heater. Several cold blow tests were made blowing air through the heater with and without the swirl injection installed. The heater pressure and air mass flow rate were recorded for each configuration. The swirl flow in the heater was found to reduce the mass flow rate by approximately 20% for fixed heater stagnation pressures. Thus, the swirl flow reduces the effective throat size for ambient air temperatures. The same effects should be present with the arc heater operating, but the magnitude could not be directly measured since the swirl is required to stabilize the arc during normal operation. Since the effective throat diameter appears in the equilibrium sonic flow equation to a power of about 5, a small error in this parameter will give gross errors in the enthalpy calculated by this equation. Thus any correlation between this method and the true stagnation enthalpy is strictly fortuitous and should not be used for this type of arc heater.

c. Stagnation Point Heating Rate Method

The total enthalpy can also be calculated from measurements of the stagnation point heat transfer rate and pitot pressure by using a theoretical equation relating these quantities. The theoretical determination of the aerodynamic heating rates for high enthalpy flows is complicated because of the large amount of dissociation energy that can become "tied up" or frozen in the flow. If complete recombination of the atoms does not occur, the measured heating rate and consequently the enthalpy will be considerably reduced. Tests described in the preceeding section have shown, however, that for these test conditions, the probe surface was catalytic to recombination, and the majority of the dissociation energy was recovered. Total enthalpy of the flow was determined by combining the pitot pressure and heat transfer rates with equilibrium heating rate theory. The theoretical equation of Fay and Riddell (Reference 16) relating the heat transfer rate and the total enthalpy for a full catalytic wall was used in the calculations.

$$H_{F\&R} = h_w + \frac{\dot{q}\sqrt{R}}{0.906 P_r^{-0.6} (\rho\mu)_w^{0.1} (\rho\mu)_s^{0.4} \left[1 + (Le^{0.52} - 1) h_d / H_o\right] (P_{T_2} / \rho_{T_2})^{0.25}}$$

The transport properties were evaluated using the real gas approximations of Hansen (Reference 17). In addition to the gas chemistry and wall catalytic effects, studies reported in Reference 18 indicate that the heating rates can also be influenced by free stream turbulence. These effects are not fully understood and the best analysis available cannot be used to obtain quantitative results. Thus, when the stagnation point heating rate method is used to determine the flow total enthalpy an independent measurement should be made with which to corroborate the results.

d. Discussion of Results

The total enthalpy profiles were highly peaked for some operating conditions and follow the same trends as the heat transfer distributions. Enthalpy profiles shown in Figure 22 for the 72-inch electrode configuration show that peaking can produce center line enthalpies almost three times higher than heat balance values. Enthalpy profiles for the 96-inch electrode shown in Figure 23 were flat up to a pressure of approximately 1000 psi. Further increases in pressure cause the enthalpy profile to peak near the center of the flow. The maximum increase in center line enthalpy for this arc heater configuration was 40% above the heat balance enthalpy. The peaked enthalpy profiles did not follow a consistent trend as is exemplified by the surveys at 1140 psi and 1310 psi. Thus, duplicating the arc heater geometry and pressure in the operating range where peaking occurs will not give repeatable center line conditions.

Center line and heat balance enthalpy measurements are summarized in Figure 24 and show the effects of pressure and front electrode length. The data for the 72-inch electrode show that the peaking starts at approximately 600 psi and the center line enthalpy is scattered depending on many factors including rear coil position and electrode surface condition. The center line enthalpy peaking for the 96-inch electrode did not become significant until the pressures exceeded 1000 psi. Below this pressure the data could be consistently repeated to within 5% or less.

The enthalpy peaking is most likely caused by the arc approaching the nozzle throat and not allowing sufficient mixing length for the hot gas. The peaking starts when the arc termination is about 10 electrode diameters from

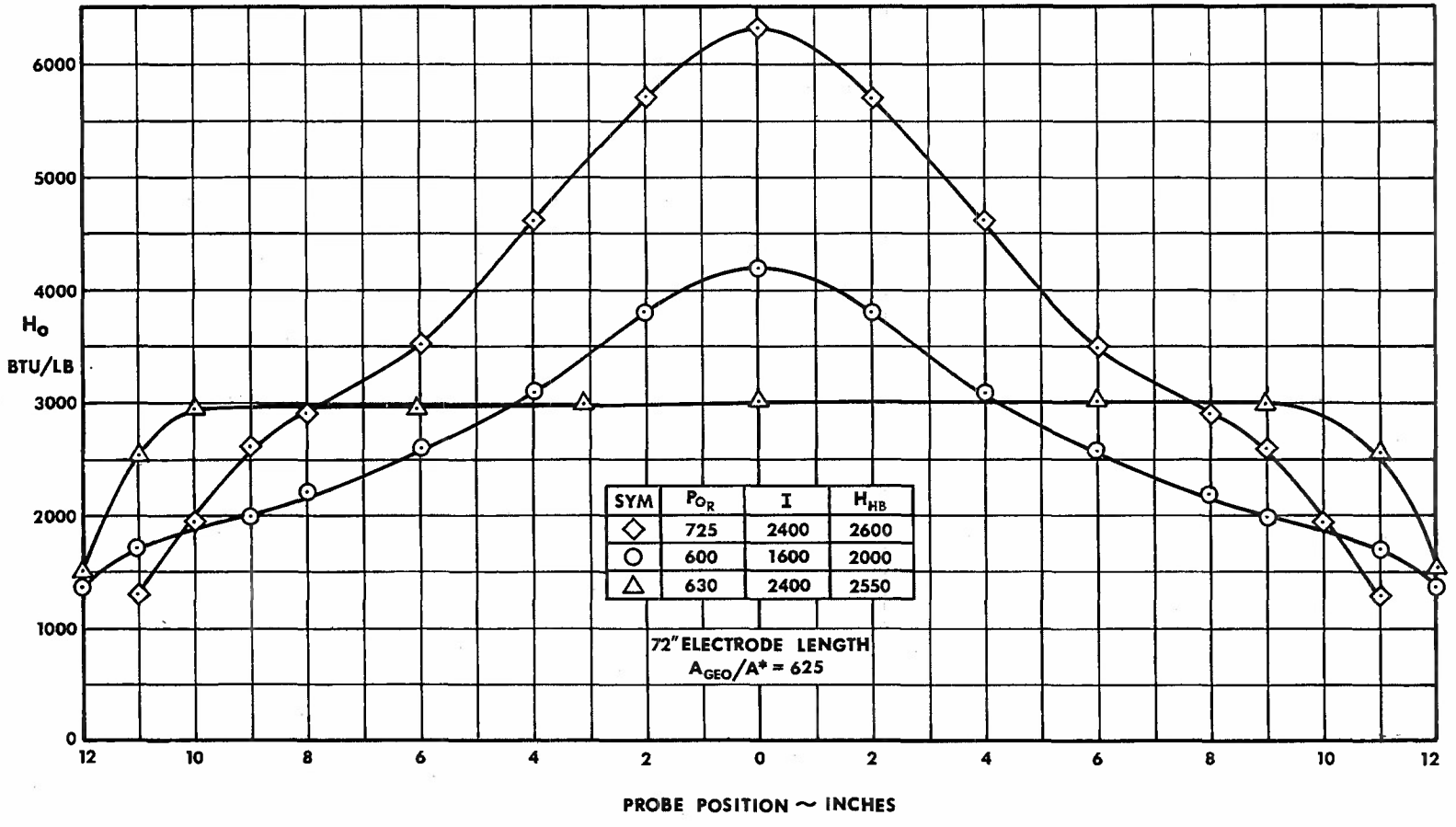

Figure 22. Total Enthalpy Profiles Showing the Effects of Pressure and Operating Currents With 72" Electrode

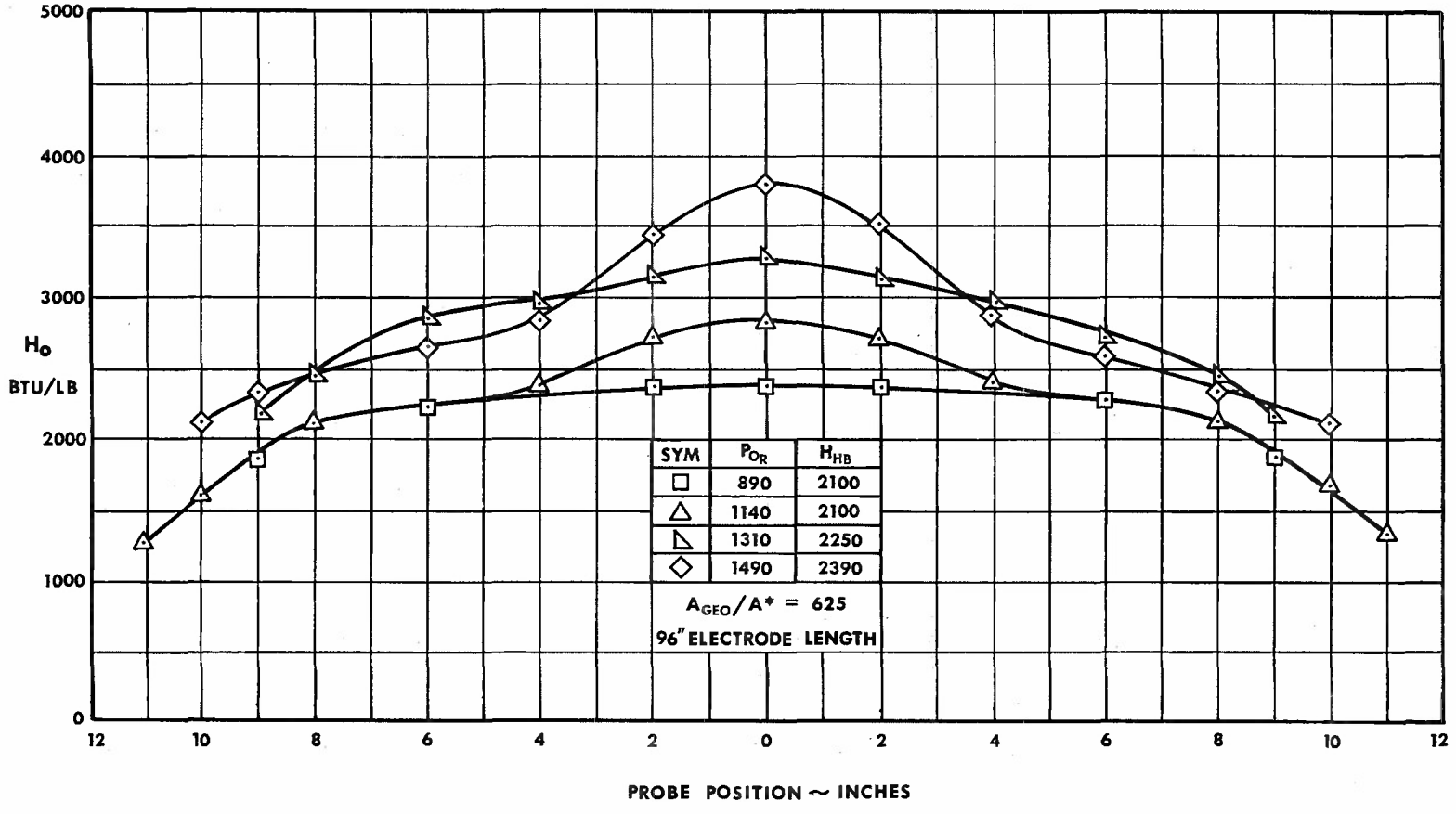

Figure 23. Total Enthalpy Profiles at Various Stagnation Pressures, With 96" Electrode

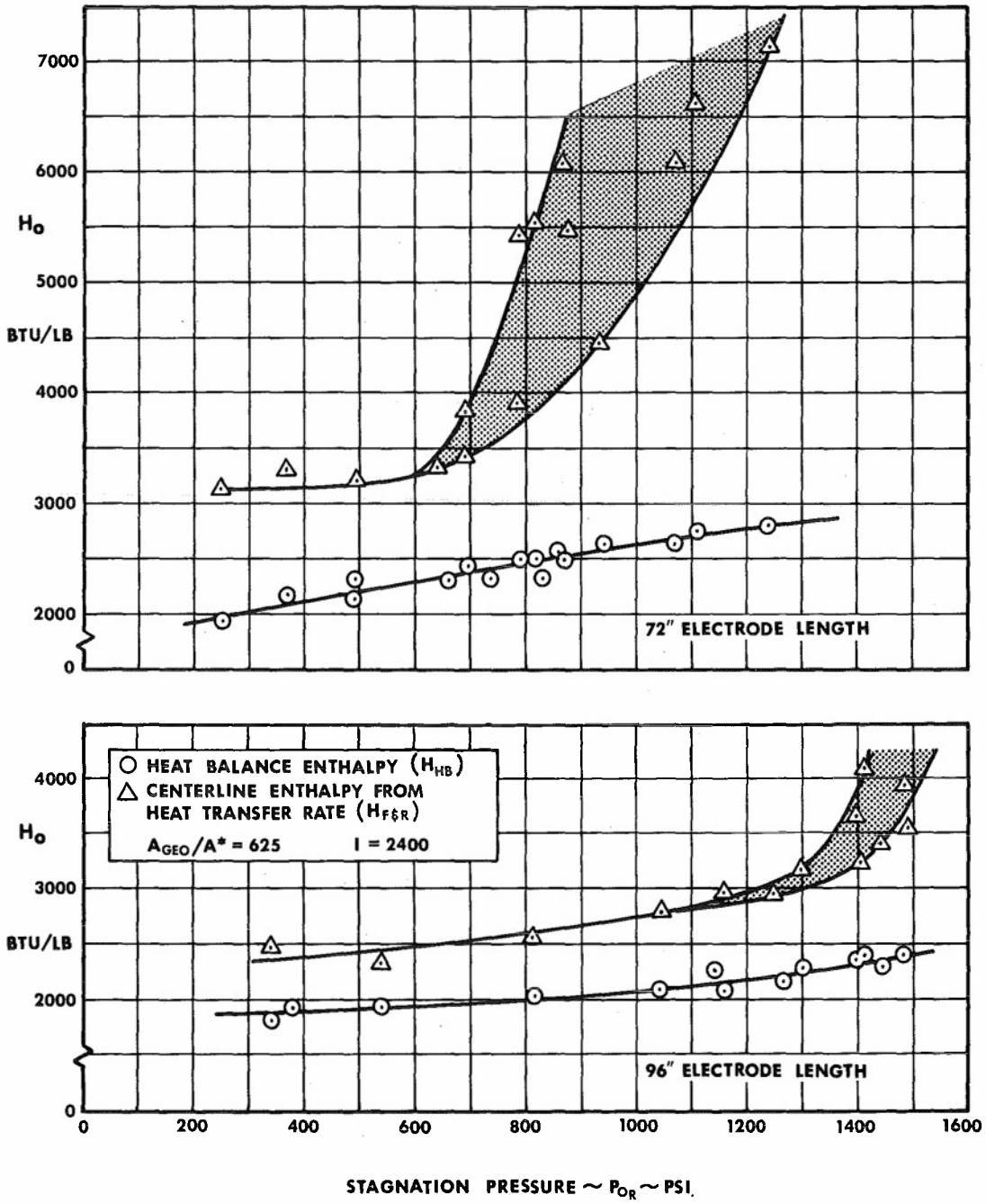

Figure 24. Total Enthalpy Measurements With 72" and 96" Electrodes

the throat and continues until the arc blows through the nozzle throat. The longer electrode configurations resulted in a more uniform temperature distribution and subsequently reduced the center line enthalpy. This increased length, however, reduced the data scatter and increased the pressure capability without a large decrease in the heat balance enthalpy. The overall effect of the increased electrode length was to significantly improve the flow uniformity and the arc heater high pressure capability.

The enthalpy calculated from the heat transfer-pitot probe measurements and the heat balance enthalpy were found to be consistent. The enthalpy surveys from the heat transfer probe can be combined with the mass flux profiles to give an average or bulk enthalpy defined by

$$\langle H \rangle = \frac{2\pi}{\dot{\omega}} \int_0^R H \rho u r \, dr$$

This equation was numerically integrated for several varied profile shapes and operating conditions with the results summarized below.

Electrode Length (in.)	P_{O_R}	I	H_{F+R} Center Line	H_{HB}	$\langle H \rangle$
96	890	2400	2410	2080	2150
96	1490	2400	3790	2390	2160
45	430	4000	4930	3350	3340
45	630	3200	4480	3390	3210

Comparing the integrated and heat balance enthalpies shows that favorable agreement was obtained between these two independent measurements.

5. FLOW BLOCKAGE STUDIES

The diffusers designed for the facility were based on criteria determined through small scale testing in a one-megawatt protype arc tunnel. Details

of the small scale tests are described in Reference 19. The "standard" blockage models chosen for diffuser performance evaluation were 60° blunted cones. Figure 25 shows a typical blockage model in the 25-inch nozzle. The models were made of laminated hard maple which formed a char layer within a few seconds of exposure to the hot flow, thus retaining their shape for long periods of time.

Figure 26 shows the sequence of events which occur when a large model blocks the flow. At zero time, the flow is fully expanded around the model. As time increases, the model wake suddenly expands and the diffuser shock moves forward toward the model closing the flow around the model. The hypersonic wake is properly shaped when the flow is fully expanded. The blocking model caused the flow to collapse more gradually with the telltale signs of the wake opening and the flow rhombus closing in.

The actual diffuser pressure recovery is compared to the small scaled tunnel data and is presented in Figure 27. The basic tunnel configuration was very near the same, the primary difference being the large size. The data curve is for a diffuser length-to-diameter ratio of 22. The large tunnel data actually showed a slightly better performance than the small tunnel, particularly with no models or small models installed. These data show that a blunt model with a base diameter of 43% of the nozzle exit diameter can be tested in the facility.

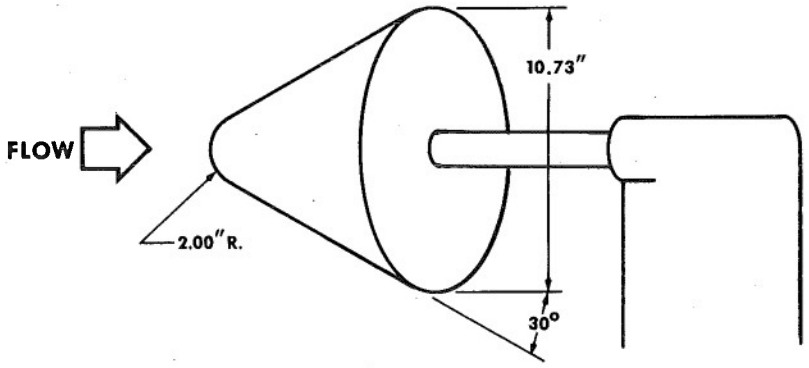

18.42% BLOCKAGE

LARGE STANDARD BLOCKAGE MODEL CONFIGURATION

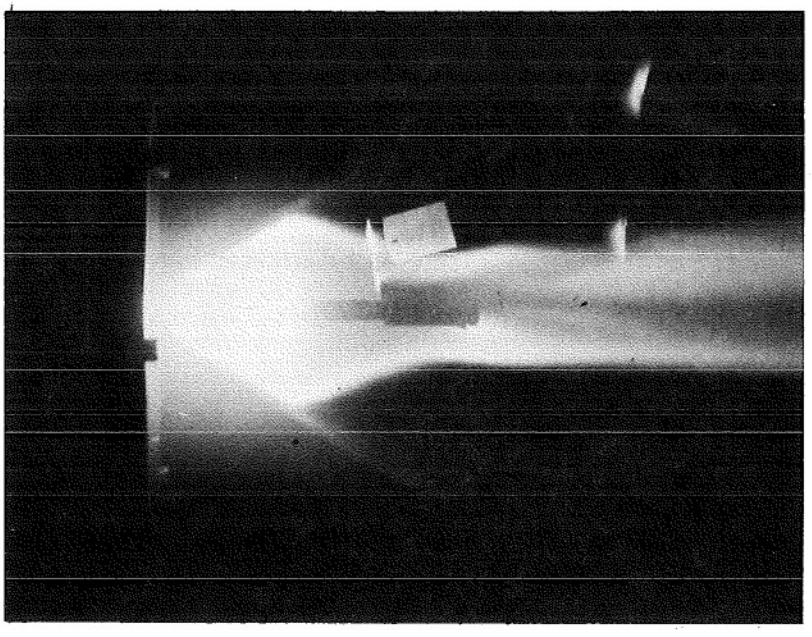

MODEL IN FLOW

Figure 25. Standard Blockage Model in Flow

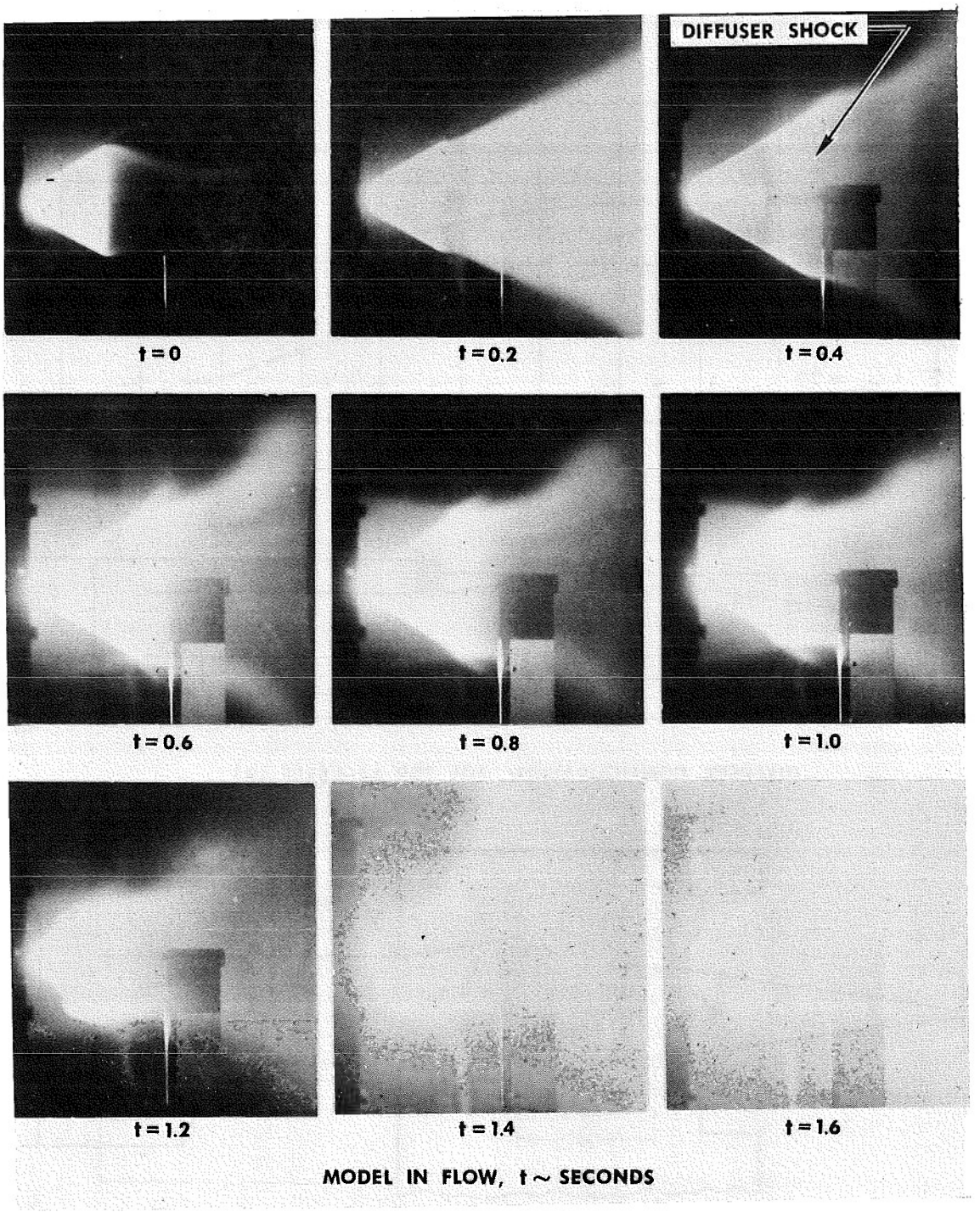

Figure 26. Sequence Photographs of Flow Blockage

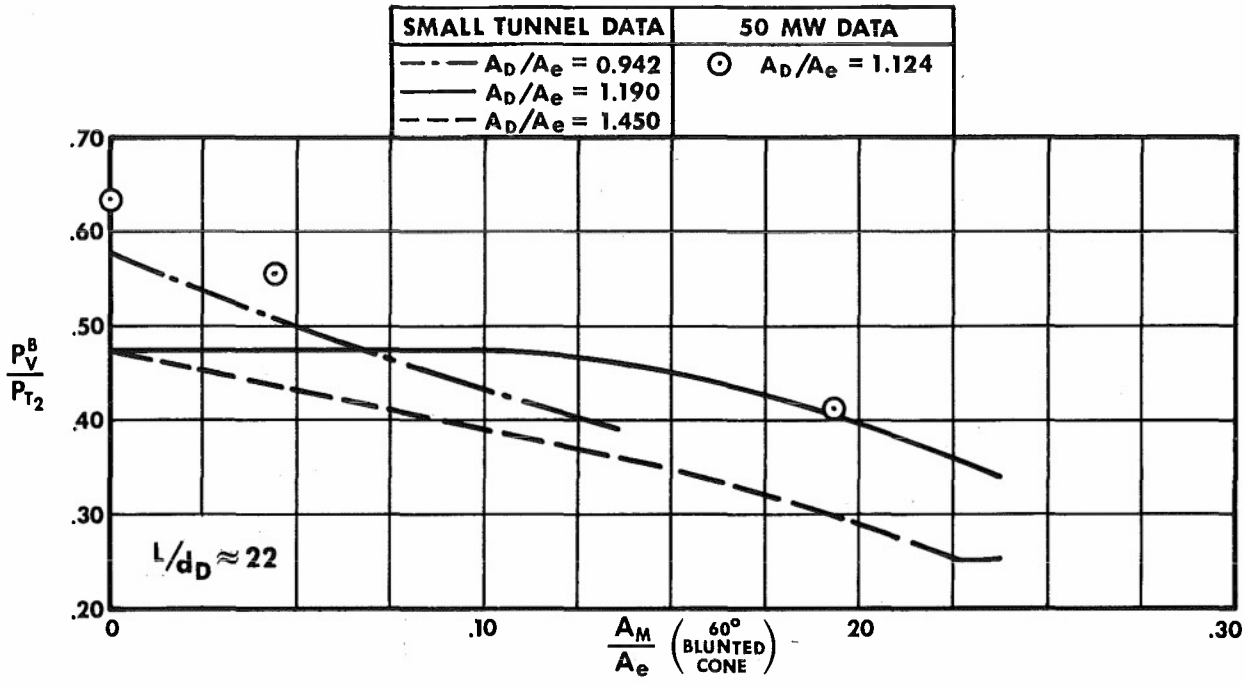

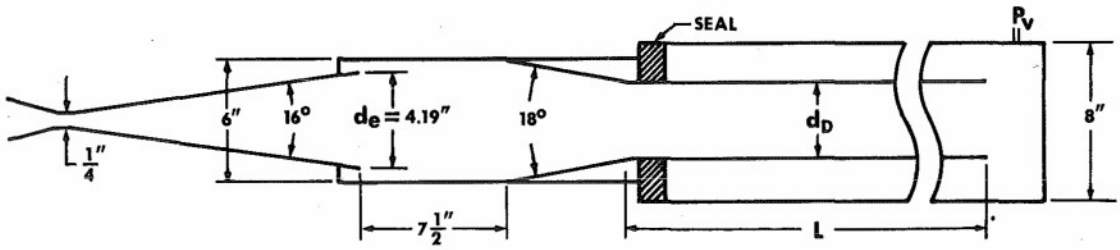

DIFFUSER CONFIGURATION, FDL TDR 64-4 (REF. 19)

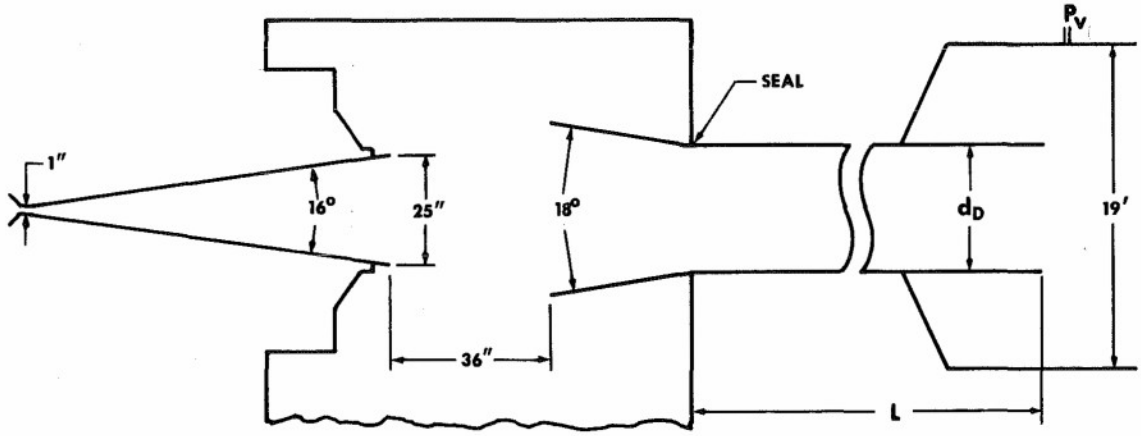

50 MEGAWATT DIFFUSER CONFIGURATION

Figure 27. Diffuser Pressure Recovery and Maximum Model Size

SECTION IV

COMPARISON OF EXPERIMENTAL RESULTS WITH THEORY

1. THEORETICAL ANALYSIS

To compare the experimental results of this investigation with theoretical predictions, several calculations were performed with the aid of a 7094 computer using a real gas nozzle expansion program. The flow model for these calculations tailored after the work of Yoshikawa and Katzen (Reference 20) assumes steady-state, one-dimensional flow that is expanded from a given set of reservoir conditions (H_0, P_0) either isentropically or in a predetermined chemically frozen state.

a. Equilibrium Expansion

The conservation equations for the isentropic expansion are given by:

$$\text{Mass: } \rho^* u^* / \rho u = A/A^* = \text{const}$$

$$\text{Energy: } H_0 = h + u^2/2 = \text{const}$$

$$\text{Entropy: } S_0 = S = \text{const}$$

and the equation of state:

$$P = \rho RT(1 + \alpha)$$

where α is the degree of dissociation. A computer program for the equation of state in canonical form developed by Lewis and Burgess (Reference 21) was used in the calculations.

b. Frozen Expansion

The high stagnation temperature achieved in the arc heater produces a substantial degree of dissociation of the gas. As the dissociated gas expands in the nozzle the recombination reaction rates cannot accomodate the large gradients in temperature and pressure thus producing a nonequilibrium gas state. Experiments (References 1 and 22) have shown that an equilibrium expansion of a high temperature gas can only be achieved for a very restricted

range of reservoir conditions. Thus, a nonequilibrium expansion process must be considered as the general case. A simplified nonequilibrium model can be obtained by assuming that the chemical composition of the gas is fixed (or frozen) at some particular state. Under these conditions the equation of state becomes:

$$P/\rho T = R(1 + \alpha_f) = \text{const}$$

Where α_f is the frozen degree of dissociation which was assumed fixed at the nozzle throat. The isentropic exponent (γ_f) was then calculated from:

$$\gamma = \frac{7 + 3\alpha_f}{5 + \alpha_f}$$

The static enthalpy term (h) in the energy equation for this case becomes:

$$h = h_f + C_{P_f}(T_f - T)$$

and the velocity is given by:

$$u = \left[2(h_o - h_f) + C_{P_f}(T_f - T)\right]^{1/2}$$

Also since γ_f = const the state variables are calculated from:

$$\frac{P}{P_f} = \left(\frac{T}{T_f}\right)^{\frac{\gamma_f}{\gamma_f - 1}}$$

Low density facilities of this type are characterized by thick boundary layers on the nozzle wall. From the pitot pressure surveys, it can be noted that the boundary layer at the nozzle exit is approximately three to four inches thick. If the boundary layer displacement thickness is not included in the analysis, the effective expansion area ratio can be in error by approximately 30%. Therefore, the boundary layer displacement thickness must be included in the analysis when comparing these experimental data with inviscid flow expansion calculations.

An iteration routine was used, alternately calculating the expansion properties and then the displacement thickness. The assumed inviscid exit diameter was corrected using the calculated value of the displacement thickness and the expansion was then recalculated. This process was continued until convergence was obtained.

2. BOUNDARY LAYER THICKNESS DETERMINATION

The boundary layer displacement thickness was calculated in this program using an empirical expression developed by Burke and Bird (Reference 23):

$$\delta^* = 0.49L \left(\frac{\rho_f u L}{\mu_f}\right)^{-0.3}$$

where the density and viscosity were evaluated at the Eckert reference enthalpy (Reference 24) given by

$$h_r = 0.22 h_o + 0.5 h_w + 0.28 h_\infty$$

Several more recent formulas and techniques for calculating displacement thicknesses have been formulated (References 4, 25, and 26) in an attempt to provide a better curve fit over a wider range of test conditions. For the Mach number and Reynolds number ranges covered in these tests, however, these differences are minimal and Burke's equation is adequate.

To provide a rough check on the validity of this boundary layer correction, several mass flux profiles were numerically integrated to obtain the boundary layer displacement thicknesses at the various operating condition. The results of these integrations are compared with Burke's correlation formula in Figure 28. The scatter of some of these data points can be attributed to the relatively large mass flux probe and the large spacing between data points. These data points were typically one inch apart in a four-inch thick boundary layer.

3. CORRELATION OF NOZZLE EXIT PRESSURES

The nozzle expansion program was run for reservoir conditions consisting of enthalpies ranging from 2000 to 4000 BTU/lb and stagnation pressures from

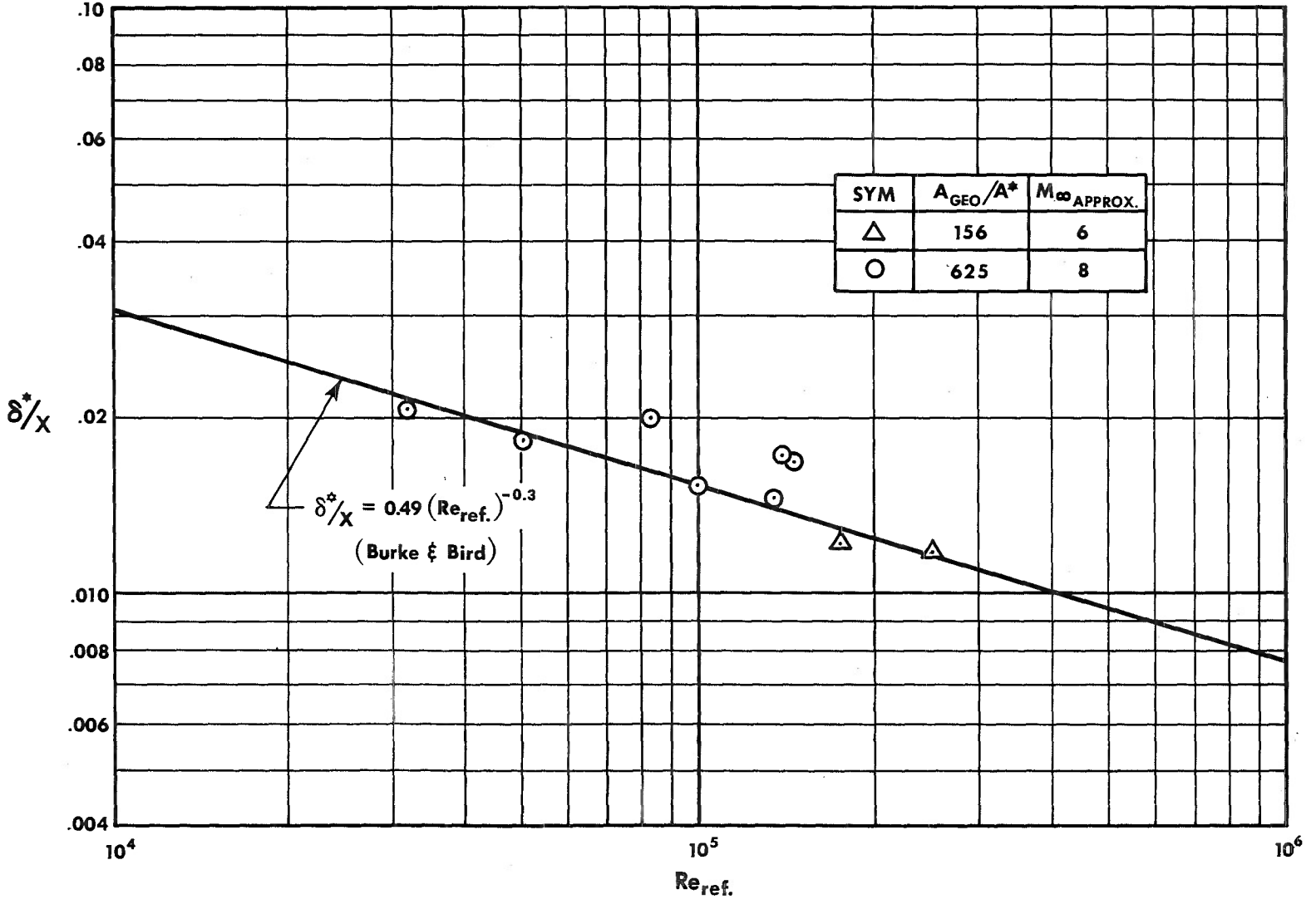

Figure 28. Correlation of Displacement Thickness Data

200 to 1400 psi. The 25-inch nozzle exit diameter and throat diameters of one and two inches gave geometric area ratios of 625 and 156, respectively. Expansions based on these assumed reservoir conditions and nozzle geometries were calculated for equilibrium and frozen flow models. The results are compared with pitot pressure and static pressure measurements in Figures 29 through 32.

Pitot pressure calculations are shown to be relatively insensitive to the flow model employed and therefore cannot be used to determine the chemical state of the gas. Center line pitot pressure measurements shown in Figures 29 and 30 correlated well with the stagnation pressure and were independent of all other operating parameters. A straight line fairing through these data was made with a mean deviation of less than 1%.

Departures from equilibrium in the expansion process can cause large differences in nozzle exit static pressures. Wall static pressures were measured over a range of reservoir pressures and are compared with theory in Figures 31 and 32. The experiments with the two-inch throat ($A/A^* = 156$) were limited to reservoir pressures less than 500 psia due to mass flow limitations. The one-inch throat experiments ($A/A^* = 625$) were conducted from reservoir pressures from 300 to 1500 psia. In the pressure range from 100 to 500 psi the data fall between the equilibrium and frozen flow theory. Since the chemistry was assumed frozen at the throat, the data indicate that the nonequilibrium starting point is downstream of the throat. No attempt was made to adjust the nonequilibrium starting point, as is usually employed in this type analysis; however, this technique would bring the data and theory into closer agreement. For reservoir pressures in excess of 500 psi the nozzle exit static pressures were in good agreement with equilibrium expansion theory. Shock tunnel experiments reported by Nagamatsu (Reference 22) gave almost identical results.

Measurements of the various flow parameters were also made at several axial locations downstream of the nozzle exit and are summarized in Figure 33. These data exhibited typical conical expansion characteristics with a 1.7% per inch pitot pressure decrease along the test section axis.

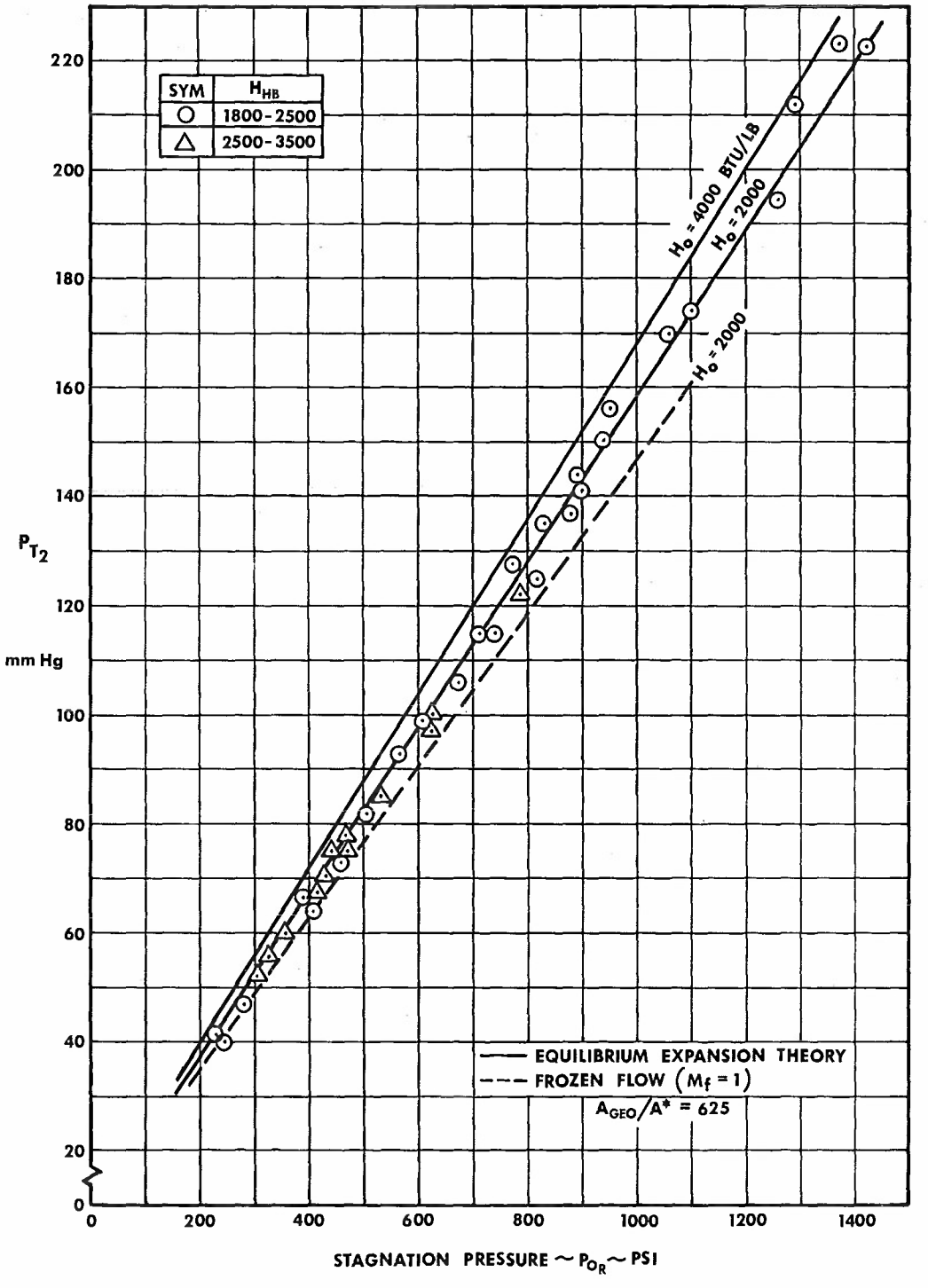

Figure 29. Comparison of Typical Center Line Pitot Pressure With Theory (d* = 1.0)

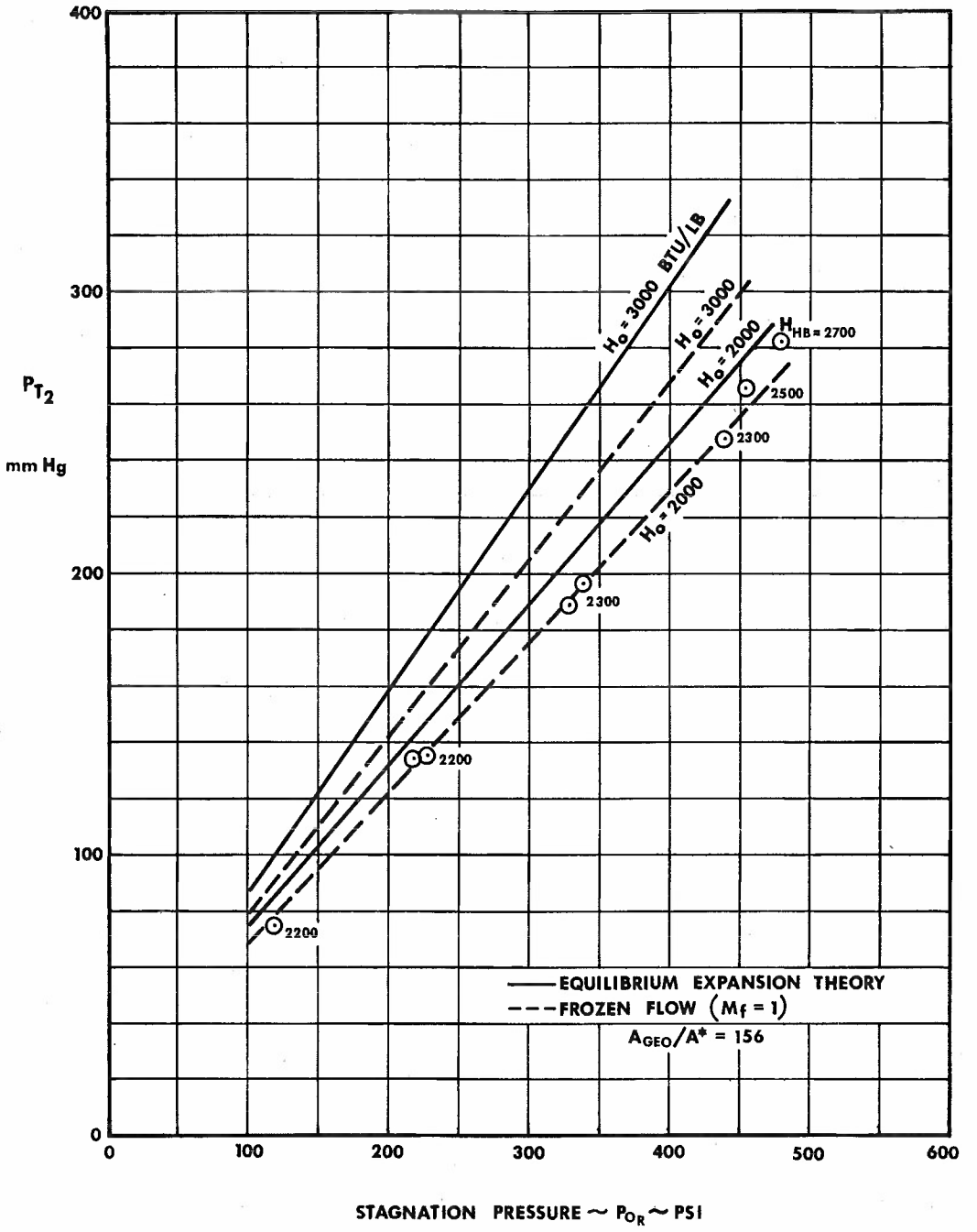

Figure 30. Comparison of Typical Center Line Pitot Pressure Measurements With Theory (d* = 2.0)

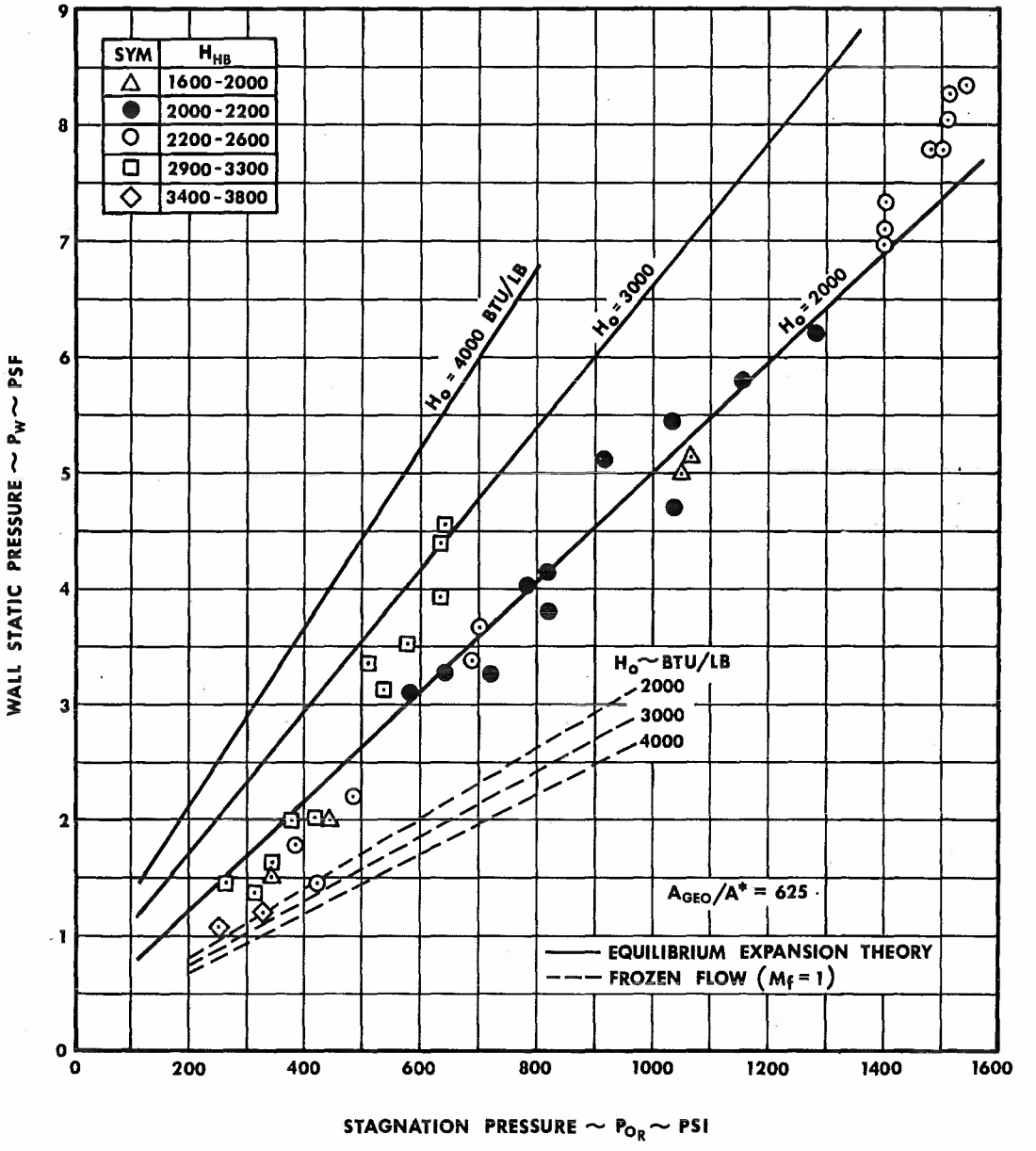

Figure 31. Comparison of Nozzle Wall Static Pressure Measurements With Theory (d* = 1.0)

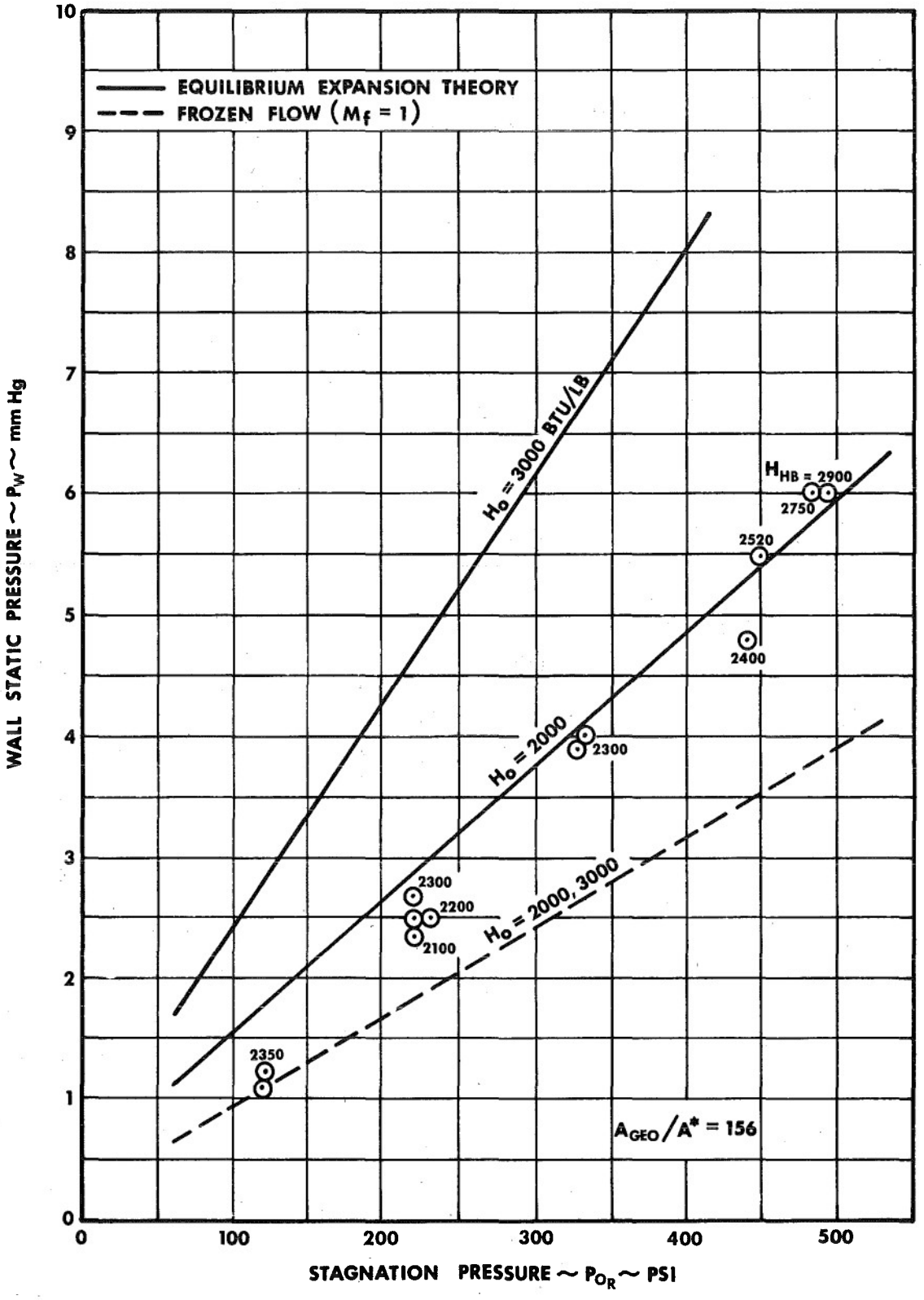

Figure 32. Comparison of Nozzle Wall Static Pressure Measurements With Theory (d* = 2.0)

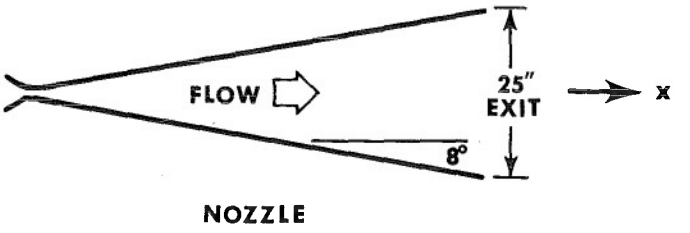

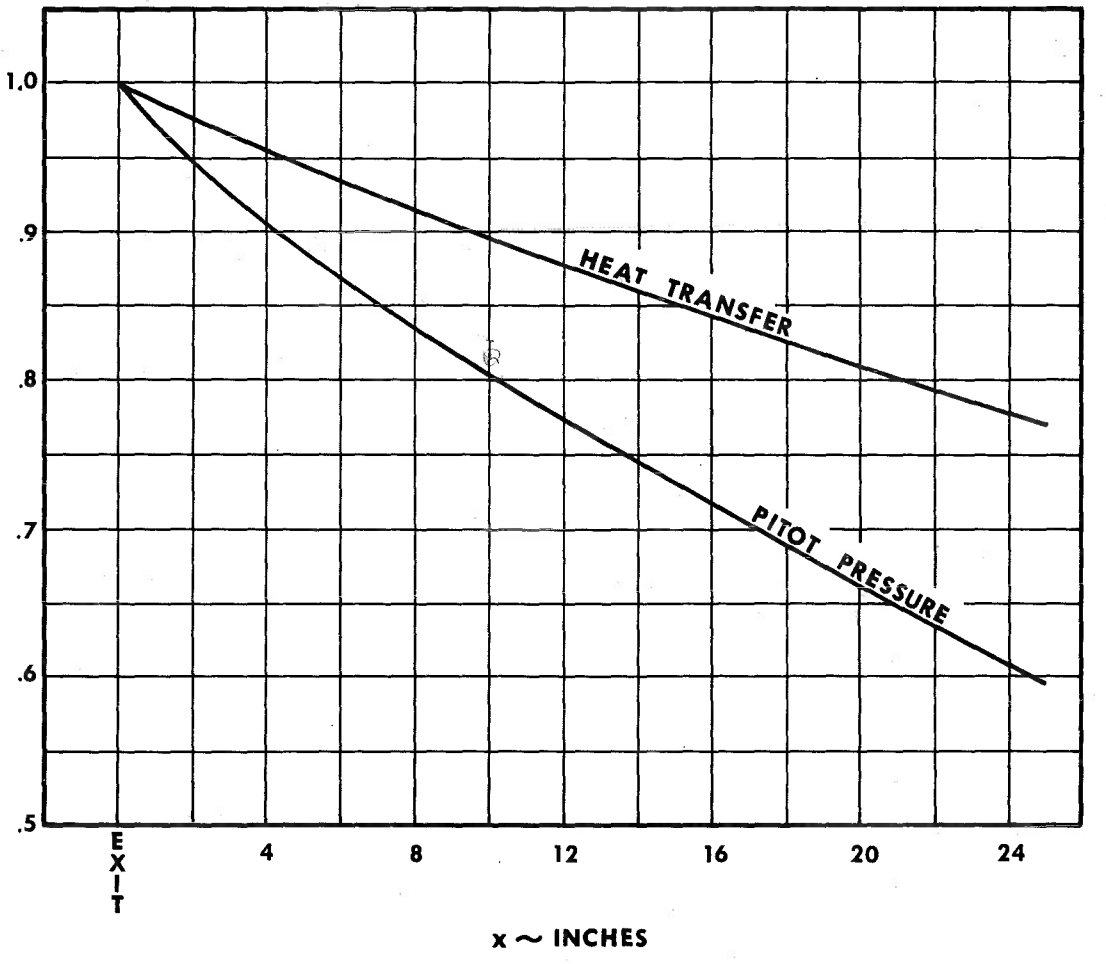

Figure 33. Representative Axial Surveys of the Ratio of Local Centerline Conditions to Exit Center Line Conditions

SECTION IV

CONCLUSIONS

These investigations have shown that for the range of conditions tested, the standard hypersonic flow diagnostic measurements of pressure, mass flux and heat transfer rate are adequate for determining the flow uniformity and the gross thermochemical state of the gas. The radial flow surveys were of major importance in assessing the flow quality and therefore must be included in the flow field calibration of any arc heated wind tunnel. The pitot pressure and mass flux measurements alone can give an inaccurate picture of the flow uniformity. These data must be accompanied by a local measurement of the stream temperature or enthalpy to completely describe the flow field.

From the three independent enthalpy measurement techniques which were evaluated, it can be concluded that the heating rate method can be successfully used in a high pressure air heated wind tunnel to determine the local total enthalpy of the expanded flow. The sonic throat method of enthalpy determination was critically analyzed for a vortex stabilized arc heater and shown to be susceptible to large errors due to the strong swirl flow which exists at the throat. The experimental expanded flow data were found to be in good agreement with one-dimensional real gas flow analysis when the appropriate reservoir conditions are used and boundary layer corrections are applied. Using the heat balance enthalpy and arc heater pressure as the reservoir conditions, the nozzle exit pressures correlated even when the enthalpy profiles were highly peaked.

For reservoir enthalpies from 2000 to 2500 BTU/lb and heater pressures in excess of 500 psi, the expanded flow data were in good agreement with equilibrium expansion theory. The nozzle data exhibited nonequilibrium expansion characteristics when the pressure was reduced below 500 psi.

Although the peaked enthalpy distribution is usually not desirable for most test programs, it can be used advantageously for blunt body testing to duplicate high stagnation region heat transfer rates. In this operating

mode center line enthalpy three times higher than bulk values were measured in the flow. The severe peaking can be suppressed for aerodynamic model testing by simply lengthening the front electrode.

REFERENCES

1. D. Zonars, "Nonequilibrium Regime of Airflows in Contoured Nozzles: Theory and Experiment," AIAA J, Vol 6, No. 1, January 1967.

2. J. A. Lordi and R. E. Mates, "Nonequilibrium Expansions of High Enthalpy Airflows," ARL-64-206, Aeronautical Research Laboratory, Wright-Patterson Air Force Base, Ohio, November 1965.

3. H. S. Dresser, E. P. French, and H. G. Webb, Computer Program for One-Dimensional Nonequilibrium Reacting Gas Flow, AFFDL-TR-67-75, Air Force Flight Dynamics Laboratory, Wright-Patterson Air Force Base, Ohio, August 1967.

4. A. F. Burke and J. E. Wallace, Aerothermodynamic Consequences of Nozzle Nonequilibrium, AEDC-TR-66-47, Arnold Engineering Development Center, Arnold Air Force Station, Tennessee, February 1966.

5. W. M. Van Camp, et al., "Study of Arc-Jet Propulsion Devices," NASA CR-54691, March 1966.

6. J. L. Potter, et al., Gasdynamic Diagnosis of High-Speed Flows Expanded From Plasma States, AEDC-TDR-63-241, Arnold Engineering Development Center, Arnold Air Force Station, Tennessee, November 1963.

7. A. Witte, T. Kubota, and L. Lees, "Experimental Investigation of a Highly Ionized Arc-Heated Supersonic Free Jet," AIAA Paper No. 68-135, January 1968.

8. R. B. Pope, "Measurements of Enthalpy in Low-Density Arc-Heated Flows," AIAA J, Vol 6, No. 1, January 1968.

9. Air Force Flight Dynamics Laboratory, "Fifty Megawatt Electrogasdynamics Facility," Wright-Patterson Air Force Base, Ohio, April 1967.

10. R. T. Smith and R. E. Stewart, "Preliminary Results of a Nominal 16 Megawatt Arc Heater Operating at High Powers and Pressures in the AFFDL 50 Megawatt Hypersonic Facility," FDM-TM-68-1, Air Force Flight Dynamics Laboratory, Wright-Patterson Air Force Base, Ohio, March 1968.

11. R. T. Smith and J. L. Folck, Operating Characteristics of a Multi-Megawatt Arc Heater Used With the AFFDL 50 Megawatt Facility, AFFDL TR-69-6, Air Force Flight Dynamics Laboratory, Wright-Patterson Air Force Base, Ohio, 1969.

12. F. J. A. Huber, "Probes for Measuring Mass Flux, Stagnation Point Heating, and Total Enthalpy of High Temperature Hypersonic Gas Flows," AIAA Paper No. 66-750, September 1966.

REFERENCES (CONTD)

13. W. L. Hankey, R. D. Neumann, and E. H. Flinn, Design Procedures for Computing Aerodynamic Heating Rates at Hypersonic Speeds, WADC TR 59-610, Wright Air Development Center, Wright-Patterson Air Force Base, Ohio, July 1960.

14. R. Goulard, "On Catalytic Recombination Rates in Hypersonic Stagnation Heat Transfer," Jet Propulsion, 28, pp. 737-745, 1958.

15. W. Winovich, "On the Equilibrium Sonic-Flow Method for Evaluating Electric-Arc Air-Heated Performance," NASA D-2132, March 1964.

16. J. A. Fay and F. R. Riddell, "Theory of Stagnation Point Heat Transfer in Dissociated Air," JAS, Vol 25, No. 2, February 1958.

17. C. F. Hansen, "Approximations for the Thermodynamic and Transport Properties of High-Temperature Air," NASA TR R-50, 1959.

18. T. M. Weeks, "Influence of Free Stream Turbulence on Hypersonic Stagnation Zone Heating," AIAA Paper No. 69-167, January 1969.

19. R. T. Smith, Experimental Studies of High Temperature Hypersonic Diffusers, AFFDL-TR-66-48, Air Force Flight Dynamics Laboratory, Wright-Patterson Air Force Base, Ohio, May 1966.

20. K. K. Yoshikawa and E. D. Katzen, "Charts for Air Flow Properties in Equilibrium and Frozen Flows in Hypervelocity Nozzles," NASA TN D-693, April 1961.

21. C. H. Lewis and E. G. Burgess, Empirical Equations for the Thermodynamic Properties of Air and Nitrogen to 15,000°K, AEDC-TDR-63-138, Arnold Engineering Development Center, Arnold Air Force Station, Tennessee, July 1963.

22. H. T. Nagamatsu, J. B. Workman, and R. E. Sheer, "Hypersonic Nozzle Expansion of Air with Atom Recombination Present," JAS Vol 28, No. 11, November 1961.

23. A. F. Burke and K. D. Bird, "The Use of Conical and Contoured Expansion Nozzles in Hypervelocity Facilities," Cornell Aeronautical Laboratory, Report No. 112, July 1962.

24. E. R. G. Eckert, Survey on Heat Transfer at High Speeds, WADC-TR-54-70, Wright Air Development Center, Wright-Patterson Air Force Base, Ohio, April 1954.

25. E. E. Edenfield and A. H. Boudreau, "A Correlation of Boundary Layer Thickness and Displacement Thickness at Hypersonic Mach Numbers," Paper presented to the Twenty-Sixth Supersonic Tunnel Association Meeting, NASA Ames Research Center, Moffett Field, Calif., September 26-27, 1966.

REFERENCES (CONTD)

26. S. L. Petrie, "Boundary Layer Studies in an Arc-Heated Wind Tunnel," The Ohio State University Research Foundation Report No. 2033, April 1968.

UNCLASSIFIED
Security Classification

DOCUMENT CONTROL DATA - R & D

(Security classification of title, body of abstract and indexing annotation must be entered when the overall report is classified)

1. ORIGINATING ACTIVITY *(Corporate author)*
Air Force Flight Dynamics Laboratory
Wright-Patterson Air Force Base, Ohio 45433

2a. REPORT SECURITY CLASSIFICATION
NONE

2b. GROUP

3. REPORT TITLE
Calibration of the AFFDL 50 Megawatt Arc Heated Hypersonic Wind Tunnel With a Two-Foot Nozzle

4. DESCRIPTIVE NOTES *(Type of report and inclusive dates)*
September 1967 - December 1968

5. AUTHOR(S) *(First name, middle initial, last name)*
Folck, James L.
Smith, Richard T.

6. REPORT DATE	7a. TOTAL NO. OF PAGES	7b. NO. OF REFS
July 1969	67	26

8a. CONTRACT OR GRANT NO.	9a. ORIGINATOR'S REPORT NUMBER(S)
b. PROJECT NO. 1426	AFFDL TR-69-36
c. Task No. 142612	9b. OTHER REPORT NO(S) *(Any other numbers that may be assigned this report)*
d.	

10. DISTRIBUTION STATEMENT
This document has been approved for public release and sale; its distribution is unlimited.

11. SUPPLEMENTARY NOTES	12. SPONSORING MILITARY ACTIVITY
	Air Force Flight Dynamics Laboratory Wright-Patterson Air Force Base, Ohio

13. ABSTRACT

This study consisted of the experimental investigation of test flow in an arc heated hypersonic wind tunnel. These tests utilized a high voltage DC arc heater which operated at input powers in excess of 50 megawatts and provided reservoir pressures ranging from 100 to 1500 psi and bulk enthalpies from 1500 to 4000 BTU/lb. Local free stream measurements of pitot pressure, mass flux, stagnation point heat transfer rate and wall static pressures were obtained at the exit of a nominal two-foot diameter conical nozzle. Stagnation enthalpy profiles at the nozzle exit became peaked at high stagnation pressures. From these data, center line enthalpies as high as 6500 BTU/lb were indicated in the flow. Selective comparisons between one-dimensional expansion theory and experiment are presented. At a reservoir enthalpy of approximately 2500 BTU/lb and for stagnation pressure in excess of 500 psi the expanded flow data were in good agreement with equilibrium expansion theory. However, below 500 psi the data compared more closely with nonequilibrium theory with the flow frozen downstream of the nozzle throat.

DD FORM 1 NOV 65 1473

UNCLASSIFIED
Security Classification

14. KEY WORDS	LINK A		LINK B		LINK C	
	ROLE	WT	ROLE	WT	ROLE	WT
1 Arc Heater wind tunnels -- Calibration						
2 Hypersonic Wind Tunnel -- Calibration						
3 Plasma Diagnostics						
Reentry Environment						

17-03